Final Technical Report – Grant DE-FG02-06ER64235, "CIBS Solar Cell Development"

Personnel: (PI) Christopher L. Exstrom, University of Nebraska at Kearney (UNK)
Department of Chemistry, exstromc@unk.edu, (308) 865-8565

(co-PI) Scott A. Darveau, UNK Department of Chemistry

(subaward institutional PI) Rodney J. Soukup, University of Nebraska-Lincoln
(UNL) Department of Electrical Engineering

(subaward institutional co-PI) Natale J. Ianno, UNL Department of Electrical
Engineering

A. Summary of Project Goals

We proposed to fabricate and study a new photovoltaic material, copper indium boron
diselenide, $CuIn_xB_{1-x}Se_2$ (CIBS), which, to the best of our knowledge, had never been grown and
studied.   Substitution of boron for indium in $CuInSe_2$ (CIS) is expected to yield a higher
bandgap – toward the optimum 1.37 eV -- for lower concentrations of boron than either gallium
or aluminum[1,2]. This lower concentration was expected to lead to thin ordered films approaching
those of CIS. CIBS had not been previously prepared or studied because the excessively high
boiling point of boron prevents its deposition by evaporation, the classical means of producing
CIS-based solar cell films.

## B. Results from Three-Step Thin-Film Fabrication Method

$CuIn_{1-x}B_x$ thin-film alloys were deposited using planar magnetron sputtering from copper,
indium, and boron targets onto molybdenum-coated soda lime glass substrates. The copper and
indium targets were dc sputtered and the boron was rf sputtered. All depositions were
accomplished in a high vacuum system (1×10^{-6} Torr) pumped by a 500 L s^{-1} turbo molecular
pump. The substrate holder was rotated and heated between 20 and 400 ^{o}C to assure uniformity
in film thickness and elemental composition. Selenization of the films was achieved by physical
vapor deposition of atomic selenium under vacuum ($< 1\times10^{-4}$ Torr) at 250°C for 20 to 40
minutes followed by annealing of the film for 20 to 40 minutes at a higher temperature ranging
from 300°C to 580°C.

Auger electron spectroscopy (AES) analysis of completed films revealed the presence of only
copper, indium and selenium. Through X-ray diffraction (XRD) patterns (Figure 1), CIS and
$Cu_{2-x}Se$ phases were identified but no boron-containing species were found. Raman microscope
images (Figure 2) revealed the presence of small crystallites that contained B_2Se_3. This
compound is known[3] to be volatile and decompose at temperatures above 450 ^{o}C. We propose

that in the selenization and/or annealing process steps, boron segregates from the copper and indium in the film, possibly mixing with selenium to form the unstable B_2Se_3 species.
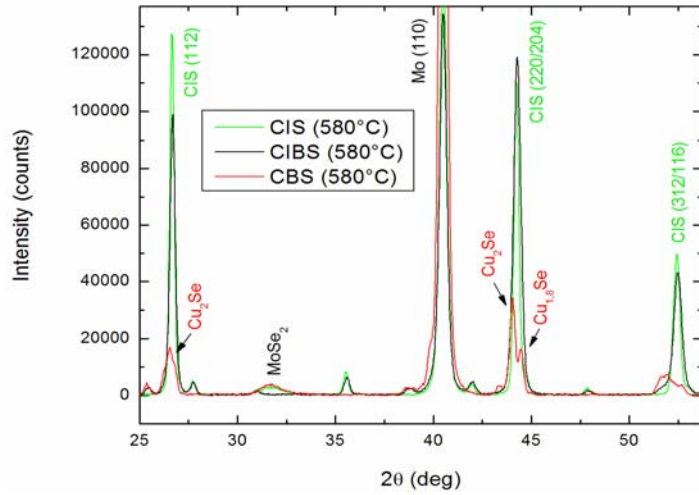

Figure 1. A comparison of XRD spectra for CIS, potential CIBS and CBS films annealed at 580 oC. No signals corresponding to boron-containing species are apparent.
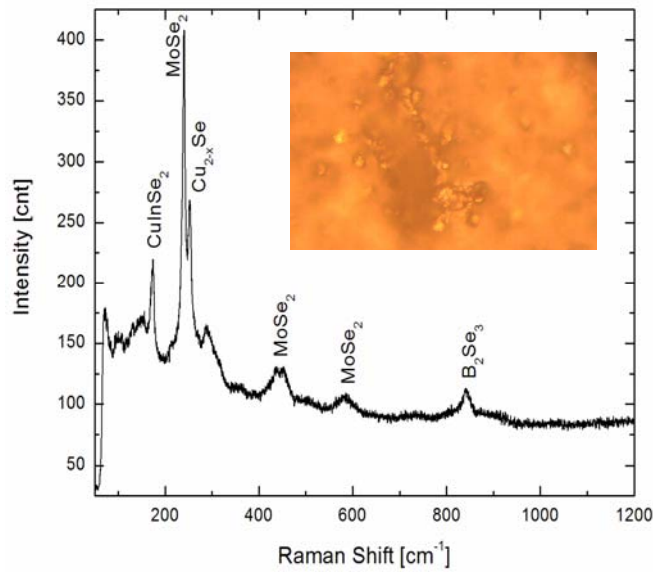
Figure 2. Raman spectrum of a surface crystallite (see optical microscope image inset) on a selenized $CuIn_{1-x}B_x$ film.

Detailed studies of the selenization of uniform $CuIn_{1-x}B_x$ alloys confirmed the boron segregation from copper and indium with accumulation at the back of the film. This behavior was observed even in films in which boron had been originally sputtered on top of $Cu_{0.45}In_{0.55}$. AES depth profiles of selenized $B/Cu_{0.45}In_{0.55}$ films (Figure 3) at temperatures ranging between 250 and 400 ^{o}C show that with increasing temperature, copper and indium migrate through the boron to the front of the film and mix with selenium forming CIS and $Cu_{2-x}Se$ species. A journal article describing these results has been accepted for publication in *Solar Energy Materials and Solar Cells*.
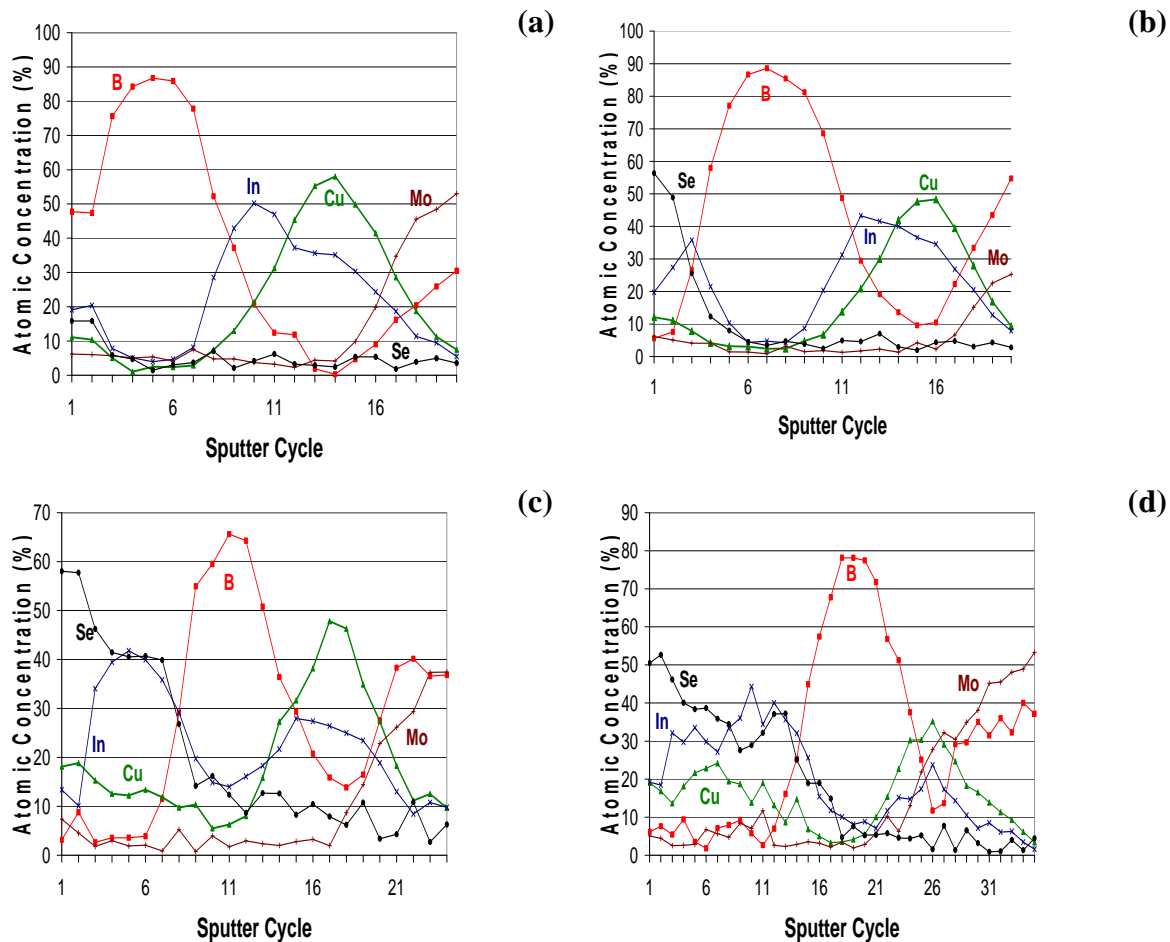
Figure 3. Auger Electron Spectroscopy depth profile of a selenized B on CuIn precursor. The procedure was halted immediately after: (a) the temperature was held at 250°C for 20 minutes; (b) a temperature ramp to 300° C; (c) a temperature ramp to 350° C; (d) a temperature ramp to 400° C.

Significance of Results and Plans for Future work: It appears that it may not be possible to form CIBS films using this three-step method. All selenized CIBS films, whether co-sputtered from individual targets simultaneously, sputtered in layers, or sputtered from composite targets lack the presence of boron in the bulk of the film. In order to more fully investigate whether CIBS films can be formed, other methods must be attempted. The next method would be to deposit the precursor films in a Se vapor as has been done successfully with aluminum[4] as the substitutional atom for indium. It may also be possible to create quality CIBS films using the hollow cathode approach[5]. Electrically excited B and Se ions that would be present in the high energy plasma may have a better chance of reacting to form B and Se bonds due to the high pressure in the nozzle[6].

C. Development of a Nanoscience-based Fabrication Method: Proof-of-Concept Studies and Preliminary Evidence of Novel CIBS Nanocrystalline Materials
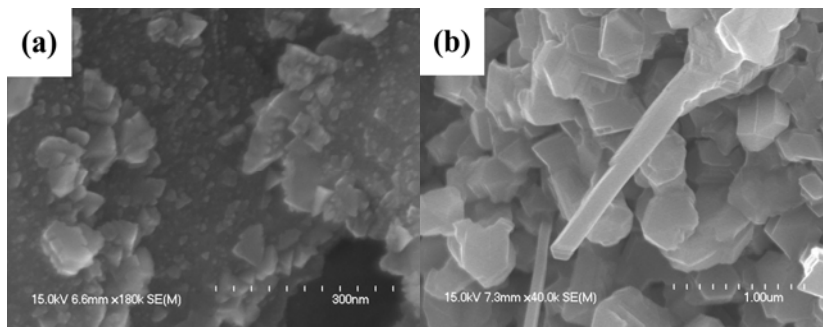
Given the difficulties of incorporating boron into the chalcopyrite material structure through the above thin-film method, a non-vacuum, chemical-based method was pursued in conjunction with chemical bath deposition method. A two-step method consisting of an open-air solvothermal reaction followed by the annealing of the resulting solid-state product at 500 $^{\circ}$C was developed, and this method shows great promise for the future preparation of CIBS nanocrystalline materials.

As a proof-of-concept study, we prepared several samples of nanocrystalline CIS, $CuIn_{1-x}Ga_xSe_2$ (CIGS), and $CuGaSe_2$ (CGS) using this two-step method. Desired stoichiometric quantities of Se, $CuCl_2$, $InCl_3$, and $GaCl_3$ were refluxed in trien for 24 (CIS) or 48 hours (CIGS, CGS). After isolation by centrifugation, rough films of the products were cast on borosilicate glass substrates from methanol and acetone suspensions. This was followed by annealing in a nitrogen atmosphere at 500 $^{\circ}$C for 20-40 minutes. Characterization data for all products after annealing are summarized in Table 1. CIGS product gallium content is directly proportional to the In/Ga mole ratio present in the reaction. SEM images of post-annealed CIGS-1 and CGS products are shown in Figure 4. These and the other chalcopyrite materials show similar morphologies consisting of mixtures of plate-like particles or large nodules (100-400 nm in diameter), nanorods (50-100 nm diameter), and clusters of spherical nanoparticles in the diameter range of 20-40 nm each. Under the annealing conditions studied, no thin-film formation was observed.

Table 1. Characterization Data for Post-annealed $CuIn_{1-x}Ga_xSe_2$ Nanocrystalline Samples

| Sample	x^a	XRD d(112), 2θ	Raman A_1 phonon, cm^{-1}
CIS	0	26.70	172
CIGS-1	0.21^b	26.74	174
CIGS-2	0.35^b	26.98	176
CIGS-3	0.79^b	27.43	179
CGS	1	27.64	185

[a] Determined by Auger spectroscopy. [b] Target x values based on starting amounts of In and Ga: 0.25 (CIGS-1), 0.50 (CIGS-2), 0.75 (CIGS-3)

Figure 4. SEM images of post-annealed (a) $CuIn_{0.79}Ga_{0.21}Se_2$ (CIGS-1 sample) and (b) $CuGaSe_2$ (CGS sample)

Employing only the solvothermal reaction step can yield nanocrystalline CIS of reasonable quality, but in CIGS and CGS preparation there is often significant $Cu_{2-x}Se$ contamination and/or the apparent presence of metal-containing precursor solids. The latter annealing step in our two-step process serves to convert precursor solids to the chalcopyrite product and improve the crystallinity of any pre-existing chalcopyrite. To the best of our knowledge, this is the first reported open-air solvothermal procedure employed in the preparation of CIGS and CGS materials. While previously reported open-air solvothermal CIS preparations involved the use of ethylenediamine (en) solvent[7], the use of the higher-boiling (267 ^oC compared to 120 ^oC for en) but chemically-similar trien appears to facilitate gallium incorporation into the nanocrystalline product structures.

We have gained information about the CIS preparation reaction pathway in trien solvent from the analysis of stable solid-state intermediates. Upon combining stoichiometric quantities of $CuCl_2$, $InCl_3$, and Se in trien, Raman peak(s) for $Cu_{2-x}Se$ (~ 255 cm^{-1}) are observable within five minutes. At this point, Se (~ 235 cm^{-1}) and $Cu_{2-x}Se$ solids are observable by Raman spectroscopy (Fig. 5a). From XRD spectroscopy, this $Cu_{2-x}Se$ phase is identified as berzelianite ($Cu_{1.8}Se$).
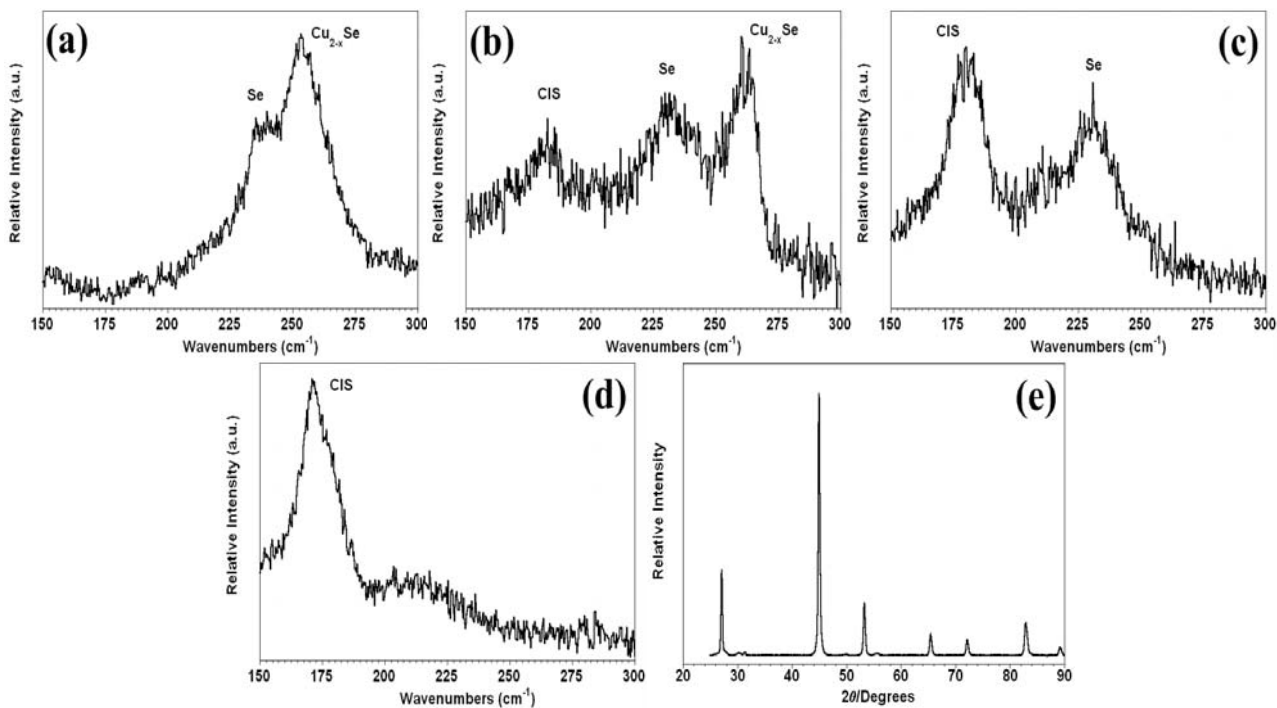


Figure 5. Raman spectra of solid products from reaction between $CuCl_2$, $InCl_3$, and Se in refluxing trien after reactions times of (a) 5 min, (b) 1 hr, (c) 6 hr, and (d) 24 hr reaction times. (e) XRD pattern of material as in (d).

No Se XRD signals appear, indicating that at this point, the Se in the sample is amorphous. As the reaction progresses, a CIS Raman peak (~ 170 cm^{-1}) starts to grow in after 1 hour (Fig. 5b). As CIS forms, the $Cu_{1.8}Se$ peak disappears within six hours (Fig. 5c). After 24 hours, all Se has

been reacted (Fig. 5d), and the XRD spectrum shows only CIS (Fig. 5e). Neither Raman spectroscopy nor XRD indicate the presence of any solid-state In species, implying that during the reaction, In exists in a soluble, ionic species.

Studies of CIGS solvothermal formation indicate that the reaction initially proceeds to CIS as described above (Figs. 5a-d) followed by a slow reaction with one or more soluble Ga species to form CIGS.

Given that solution-phase charged complexes may be important in solvothermal preparation mechanisms, it is feasible that solution ionic strength or counterion presence could affect the stability of these complexes during the reaction. $CuCl_2$, $InCl_3$, and Se were reacted in refluxing trien solvent that contained a 2- to 18-times mole excess (relative to Cu) of an ammonium or halide salt. Reaction rates are greatly accelerated. Pure CIS (as determined by Raman and XRD spectroscopy) can be prepared in as little as 30 minutes when an 18-fold NH_4Cl excess is present. This compares to 24 hours without any NH_4Cl in the reaction mixture. We propose a reaction pathway scheme (Figure 6) that features solubilization of Cu, In, Ga, and Se starting materials, rapid nucleation and growth of $Cu_{2-x}Se(s)$ particles, and subsequent reactions of these with a soluble In species, forming CIS, followed by reaction with a soluble Ga species, forming CIGS. Halide anions from added ammonium salts are believed to accelerate the reaction by limiting $Cu_{2-x}Se$ particle growth through a competitive Cu-halide complex formation step. The smaller $Cu_{2-x}Se$ particles may react faster with In to form CIS.
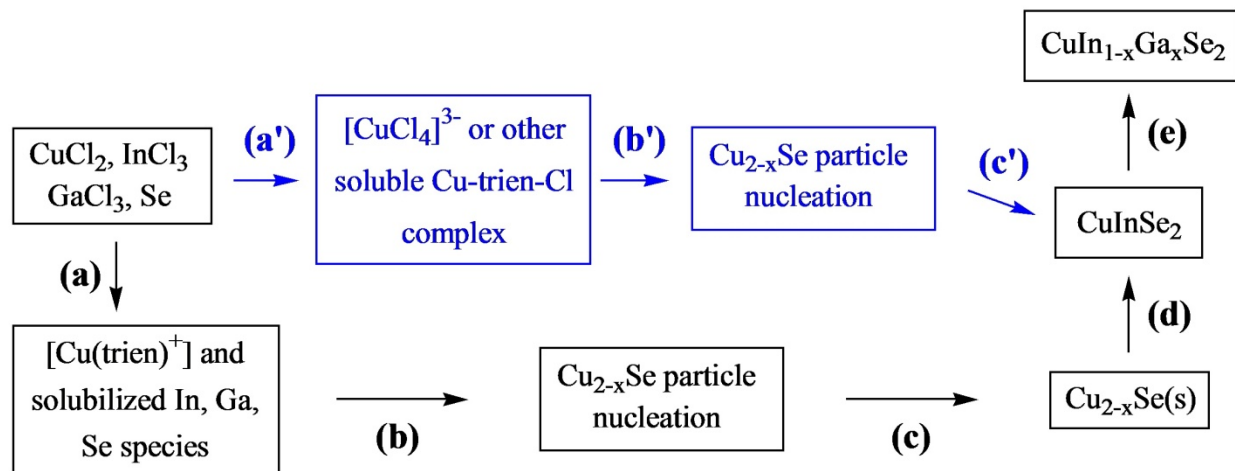
Figure 6. Proposed reaction pathway scheme for the solvothermal preparation of nanocrystalline $CuIn_{1-x}Ga_xSe_2$ in triethylenetetramine. See the text for descriptions of the lettered steps. The blue pathway steps (a'), (b'), and (c') are proposed to be adopted in place of steps (a) through (d) when NH_4Cl is present in the reaction mixture.

Results from these proof-of-concept studies indicate that incorporation of boron into a CIS chalcopyrite crystalline structure may occur more readily at the molecular- or nanoparticle-level

than in micro- or polycrystalline systems that exist in thin films. Reactions of $CuCl_2$, $InCl_3$, H_3BO_3, and Se in trien have resulted in nanocrystalline materials that, by micro-Raman spectroscopy (Figure 7), may consist of CIS/CIBS mixtures.
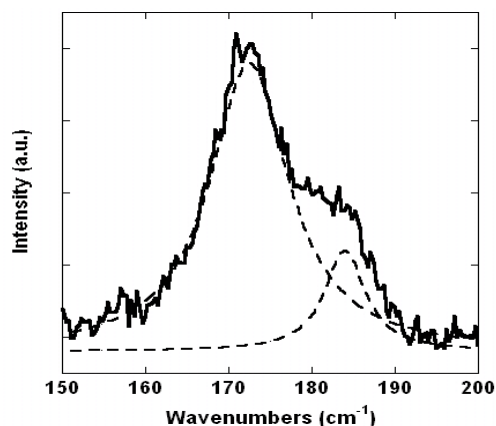
Figure 7. Raman spectrum (solid line) and 2-band deconvolution (dashed lines) of solid product from reaction between $CuCl_2$, $InCl_3$, H_3BO_3, and Se in refluxing trien solvent for 4 days. A mixture which may include $CuIn_{1-x}B_xSe_2$ appears to be present.

Future Work: In the solvothermal preparation mechanism, the control of intermediate species particle sizes may be important for the incorporation of boron into the CIS chalcopyrite crystalline structure. Surfactant-based solvents such as oleylamine, octadecylamine, and trioctylphosphine will be employed in order to optimize particle sizes during the reaction and encourage boron incorporation. This work will be supported from recent grant awards from the DOE Office of Energy Efficiency and Renewable Energy and the Nebraska Research Initiative Program.

D. References

1. Contreras, M.A.; Ramanathan, K.; AbuShama, J.; Hasoon, F.; Young, D.L.; Egass, B.; Noufi, R., "Diode Characteristics in State-of-the-Art ZnO/CdS/Cu(In$_{1-x}$Ga$_x$)Se$_2$ Solar Cells," *Prog. Photovolt: Res. Appl.* **2005**, *13*, 209-216.

2. Su-Huai Wei and Alex Zunger, "Band Offsets and Optical Bowings of Chalcopyrites and Zn-Based II-VI Allotys," *J. Appl. Phys.* **1995**, *78*, 3846-3856.

3. Hutchinson, W.E.; Eick, H.A., "Preparation and Properties of Boron Sesquiselenide," *Inorg. Chem.* **1962**, *1*, 434-436.

4. Marsillac, S.; Paulson, P.D.; Haimbodi, M.W.; Birkmire, R.W.; Shafarman, W.N., "High efficiency solar cells based on Cu(In,Al)Se$_2$ thin films", *Appl. Phys. Lett.* **2002**, *81*, 1350-1352.

5. Soukup, R.J.; Ianno, N.J.; Huguenin-Love, J.L., "Analysis of Semiconductor Thin Films Deposited using a Hollow Cathode Plasma Torch," *Solar Energy Materials and Solar Cells* **2007**, *91*, 1383-1387.

6. Z. Hubicka, personal communication.

7. Yang, Y.-H.; Chen, Y.-T., "Solvothermal preparation and spectroscopic characterization of copper indium diselenide nanorods," *J. Phys. Chem. B* **2006,** *110*, 17370-17374.

E. Publications resulting from work supported by this grant (refereed unless otherwise noted) – copies are attached at the end of this report

1. "Copper-indium-boron-diselenide Absorber Materials," Ianno, N.J.; Soukup, R.J.; Santero, T.; Kamler, C.A.; Huguenin-Love, J.L.; Darveau, S.A.; Olejníček, J.; Exstrom, C.L., *Materials Research Symposium Proceedings*, **2007**, *1012*, 151-156.

2. "Reaction Pathway Insights into the Solvothermal Preparation of $CuIn_{1-x}Ga_xSe_2$ Nanocrystalline Materials," Exstrom, C.L.; Darveau, S.A.; Martinez-Skinner, A.L.; Ingersoll, M.A.; Olejnicek, J.; Mirasano, A.; Haussler, A.T.; Huguenin-Love, J.L.; Kamler, C.A.; Ianno, N.J.; Soukup, R.J., *Proceedings of the 33rd IEEE Photovoltaics Specialists Conference*, 2008. (non-refereed)

3. "Thin Films Formed by Selenization of $CuIn_xB_{1-x}$ Precursors in Se Vapor," Kamler, C.A.; Soukup, R.J.; Ianno, N.J.; Huguenin-Love, J.L.; Olejníček, J.; Darveau, S.A.; Exstrom, C.L., *Solar Energy Materials and Solar Cells*, in press.

4. "A Non-vacuum Process for Preparing Nanocrystalline $CuIn_{1-x}Ga_xSe_2$ Materials Involving an Open-air Solvothermal Reaction," Olejnicek, J.; Kamler, C.A.; Mirasano, A.; Martinez-Skinner, A.L.; Ingersoll, M.A.; Exstrom, C.L.; Darveau, S.A.; Huguenin-Love, J.L.; Diaz, M.; Ianno, N.J.; Soukup, R.J., *Solar Energy Materials and Solar Cells*, submitted for publication.

F. Professional Conference Presentations resulting from work supported by this grant

1. "Preliminary Study of $CuIn_xB_{1-x}Se_2$ Absorber Materials," Ianno, N.J.; Santero, T.; Soukup, R.J., *53rd International Symposium and Exhibition of the American Vacuum Society*, San Francisco, CA, November 2006.

2. "Toward Fabrication and Characterization of New Photovoltaic Materials: $CuIn_xB_{1-x}Se_2$ (CIBS) and $CuBSe_2$ (CBS)," Darveau, S.A.; Olejníček, J.; Exstrom, C.L.; Soukup, R.J.; Ianno, N.J., *233rd National Meeting of the American Chemical Society*, Chicago, IL, March 26, 2007.

3. "CuIn$_x$B$_{1-x}$Se$_2$ Absorber Materials," <u>Ianno, N.J.</u>; Santero, T.; Soukup, R.J.; Exstrom, C.L.; Olejníček, J.; Darveau, S.A., *Materials Research Society Symposium*, San Francisco, CA, April 9-13, 2007.

4. "Thin Films Formed by Selenization of CuIn$_x$B$_{1\_x}$ Precursors in Se Vapor," <u>Soukup, R.J.</u>; Ianno, N. J.; Kamler, C.A.; Huguenin-Love, J.L.; Olejníček, J.; Darveau, S.A.; Exstrom, C.L., *XVI International Materials Research Congress*, Cancun, Mexico, October 30, 2007.

5. "Ionic Strength and Counterion Effects on the Solvothermal Preparation of CuInSe$_2$ Nanocrystalline Materials", <u>Martinez-Skinner, A.L.</u>; Ingersoll, M.A.; Darveau, S.A.; Exstrom, C.L. *42nd Midwest Regional Meeting of the American Chemical Society*, Kansas City, MO, November 7-9, 2007.

6. "Solid-state Intermediates in the Solvothermal Preparation of CuInSe$_2$ Nanocrystalline Materials", <u>Ingersoll, M.A.</u>; Martinez-Skinner, A.L.; Darveau, S.A.; Exstrom, C.L. *42nd Midwest Regional Meeting of the American Chemical Society*, Kansas City, MO, November 7-9, 2007.

7. "Variation in the Indium-Gallium Stoichiometry in the Solvothermal Preparation of CuIn$_{1-x}$Ga$_x$Se$_2$ Nanocrystalline Materials" Martinez-Skinner, A.L.; Ingersoll, M.A.; Olejníček, J.; Mirasano, A.; Haussler, A.T.; <u>Exstrom, C.L.</u>; Darveau, S.A.; Huguenin-Love, J.; Kamler, C.; Ianno, N.J.; Soukup, R.J., *42nd Midwest Regional Meeting of the American Chemical Society*, Kansas City, MO, November 7-9, 2007.

8. "Problems with synthesis of chalcopyrite CuIn$_{1-x}$B$_x$Se$_2$," <u>Olejníček, J.</u>; Darveau, S.A.; Exstrom, C.L.; Brown, T.; Martinez-Skinner, A.L.; Haussler, A.T.; Mirasano, A.; Ingersoll, M.A.; Ianno, N.J.; Soukup, R.J.; Kamler, C.A.; Huguenin-Love, J.L., *First International Conference on Thin Films and Porous Materials*, Algiers, Algeria, May 2008.

9. "Reaction Pathway Insights into the Solvothermal Preparation of CuIn$_{1-x}$Ga$_x$Se$_2$ Nanocrystalline Materials" <u>Exstrom, C.L.</u>; Darveau, S.A.; Martinez-Skinner, A.L.; Ingersoll, M.A.; Olejníček, J.; Mirasano, A.; Haussler, A.T.; Huguenin-Love, J.; Kamler, C.; Diaz, M.; Ianno, N.J.; Soukup, R.J., *33rd IEEE Photovoltaics Specialists Conference*, San Diego, CA, May 11-16, 2008.

10. "*Ex-situ* and *In-situ* Selenization of Copper-Indium-Boron Thin Films," <u>Soukup, R.J.</u>; Ianno, N.J.; Kamler, C.A.; Diaz, M.; Sharma, S.; Huguenin-Love, J.L.; Olejníček, J.; Exstrom, C.L.; Darveau, S.A., *33rd IEEE Photovoltaics Specialists Conference*, San Diego, CA, May 11-16, 2008.

11. "Selenization of Copper_Indium_Boron Thin Film Photovoltaic Absrober Materials," <u>Soukup, R.J.</u>; Ianno, N.J.; Kamler, C.A.; Diaz, M.; Sharma, S.; Huguenin-Love, J.L.;

Olejníček, J.; Exstrom, C.L.; Darveau, S.A., *International Union of Materials Research Societies-International Conference on Electronic Materials*, Sydney, Australia, July 2008.

12. "Solvothermal Preparation and Processing of Nanocrystalline CuIn$_{1-x}$Ga$_x$Se$_2$ Materials," <u>Kamler, C.A.</u>; Huguenin-Love, J.L.; Diaz, M.; Ianno, N.J.; Soukup, R.J.; Exstrom, C.L.; Darveau, S.A.; Martinez-Skinner, A.L.; Ingersoll, M.A.; Olejníček, J.; Mirasano, A.; Haussler, A.T., *XVII International Materials Research Congress*, Cancun, Mexico, August 2008.

G. External Grants obtained for future work

1. Exstrom, C.L. (PI); Darveau, S.A. (co-PI); Ianno, N.J. (institutional subaward PI); Soukup, R.J. (institutional subaward co-PI), "CIBS Solar Cell Development," DOE Office of Energy Efficiency and Renewable Energy, $934,800, 2008-2010.

2. Soukup, R.J. (PI); Ianno, N.J. (co-PI); Exstrom, C.L. (institutional subaward PI); Darveau, S.A. (institutional subaward co-PI), "A New Wide Bandgap Material for Semiconductor Solar Cell Materials," Nebraska Research Initiative Program, $105,000, 2006-2009.

H. Patent Certification Form OMB 1902-0121 – see attached

I. Financial Assistance Property Certification Form – see attached

J. Financial Report – see the attached SF-269

K. Copies of publications listed in Section E – see attached

PATENT CERTIFICATION

University of Nebraska at Kearney

Awardee   ☐ Interim Certification

DE-FG02-06ER64235

DOE Prime and/or Subcontract Nos.   ☒ Final Certification

Awardee hereby certifies unless indicated to the contrary, that:

1. All procedures for identifying and disclosing subject inventions as required by the patent clause of the contract have been followed throughout the reporting period.

2. There were no subcontracts or purchase orders involving research, development, and demonstration except as follows: (a separate certification must be provided to DOE for each subcontract or purchase order awarded.)

3. No inventions or discoveries were made or conceived in the course of or under this contract other than the following (Certification includes ☒, does not include ☐ all subcontracts):

TITLE	INVENTOR	DATE REPORTED	DOE "S" NO.*
none			

4. The completion date of this contract is as follows: June 14, 2008

5. The following period is covered by this certification:

May	15	2006	to June	14	2008
Month	Day	Year	Month	Day	Year

Univ. of Nebraska at Kearney

Contractor   Signature

Director, Office of Sponsored Program

Title

905 W. 25th St., Kearney, NE   _10-6-8_

Address   68849   Date of Certification

* Also include Subcontract No. if available.

NOTE: A positive certification for this Item 3 does not negate the requirement for furnishing to DOE a fully executed Patent Certification from each subawardee identified in Item 2.

FINANCIAL ASSISTANCE
PROPERTY CLOSEOUT CERTIFICATION

Award Number DE-FG02-06ER64235	Recipient *(Name and address)* Univ. of Nebraska at Kearney 905 W. 25th St., Kearney, NE 68849

The purpose of this report is to facilitate the closeout of the Award. Based on the records maintained by the Recipient in accordance with the Property Management standards set forth in the Award, the following data reflects the Recipient's closeout inventory of real and personal property that was provided by the Department of Energy (DOE) or partially or wholly acquired with project funds.

I. EQUIPMENT

A. **Federally-Owned**: *(Government Furnished Equipment): (10 CFR 600.133(a), 600.232, 600.322, or Federal Demonstration Partnership (FDP) General Terms and Conditions No. 33, as applicable):* ☒ No   ☐ Yes

*(If **yes**, attach property inventory list that includes item description, manufacturer, model, serial number, original acquisition date, original acquisition cost and disposal condition code per the Federal Management Regulation 102-36.240)*

B. **Equipment Acquired with Award Funds where Title Vests in the Recipient with further obligations to DOE:**
(10 CFR 600.133, 600.134, 600.232, or 600.321, as applicable)

☒ No   ☐ Yes

If **yes**, does the equipment have a per unit fair market value of $5,000 or more?   ☐ No   ☐ Yes

*(If **yes**, attach a property inventory list that includes item description, manufacturer, model, serial number, original acquisition date, original acquisition cost, disposal condition code per the Federal Management Regulation 102-36-240 and one of the disposition codes listed below)*

(1) The property will continue to be used for the purposes authorized in the Award.

(2) The property is no longer needed for the purposes of the Award, and will be used on another Federally sponsored activity *(List Activity and Federal Agency)*:

(3) The Recipient wishes to retain the property and compensate DOE for its share of the current per unit fair market value.

(Identify the fair market value on the attached property inventory list and describe how the value was determined).

(4) The property is no longer needed for the purposes of the Award or other Federally sponsored activities and the Recipient requests DOE disposition instructions.

II. SUPPLIES *(10 CFR 600.135, 600.233, 600.324, or FDP General Terms and Conditions No. 35, as applicable)*

Does the residual inventory of unused supplies exceed $5,000 in total aggregate value? ☐ No ☐ Yes *(if yes, check block below)*

☐ The supplies will be used on another Federally sponsored activity *(List Activity and Federal Agency).*

☐ The supplies will be sold or retained for use on non-Federally sponsored activities and the Recipient will compensate DOE for its share of the sales proceeds (or estimate of current fair market value). Attach a list of the supplies and complete the following Worksheet:

Sale proceeds or estimate of current fair market value............................	$_____
Percentage of Federal participation	_____%
Federal share	$_____
Selling and handling allowance	$_____
Amount to be remitted to DOE	$_____

FINANCIAL ASSISTANCE
PROPERTY CLOSEOUT CERTIFICATION

III. REAL PROPERTY: *(Real Estate - 10 CFR 600.132, /600.231, 600.321, or FDP General Terms and Conditions No. 32, as applicable)* ☐ No ☐Yes *(If **yes**, complete A –C)*

    A. Description of Real Property:

    B. Complete Address of Real Property:

    C. Period of Federal Interest in the Property: From _____ To _____ (Unless the award specifies otherwise, the Federal Interest in the property ends when the award project period ends.)

    D. Disposition Preference Request. If the period of Federal Interest in the property exceeds the project period, check one of the following blocks to indicate your disposition preference:

    ☐ Transfer property to another Federal award.

    ☐ Sell and compensate DOE.

    ☐ Return to DOE.

    ☐ Retain title and compensate DOE for its share of the current fair market value of the property.

Certification: I certify to the best of my knowledge and belief that all information presented in this report is true, correct and complete, and constitutes a material representation of fact upon which the Federal government may rely.

Name	Signature	Title	Date
John Falconer	*(signature)*	Director, OSP	10-6-4

FINANCIAL ASSISTANCE
PROPERTY CLOSEOUT CERTIFICATION

To be completed by the Department of Energy:

DOE PROPERTY DISPOSITION

☐ Negative Report

☐ Real Property:

☐ Equipment:

☐ Supplies:

Property Management Official Name	Signature	Date

FINANCIAL STATUS REPORT
(Long Form)

(Follow instructions on the back)

REVISED FINAL 9/29/08

OMB Approval No. 0348-0039	Page 1 of 1 pages

1. Federal Agency and Organizational Element to Which Report is Submitted
U.S. Department of Energy

2. Federal Grant or Other Identifying Number Assigned By Federal Agency
DE-FG02-06ER64235

3. Recipient Organization (Name and complete address, including ZIP code)
University of Nebraska at Kearney, 905 W. 25th Street, Kearney, NE 68849

4. Employer Identification Number	5. Recipient Account Number or Identifying Number	6. Final Report	7. Basis
47-0491233	550511005001	☒ Yes ☐ No	☒ Cash ☐ Accrual

8. Funding/Grant Period (See instructions)
From: (Month, Day, Year) 5/15/2006
To: (Month, Day, Year) 6/14/2008

9. Period Covered by this Report
From: (Month, Day, Year) 5/15/2006
To: (Month, Day, Year) 9/15/2008

10. Transactions:

		I Previously Reported	II This Period	III Cumulative
a.	Total outlays		770,000.00	770,000.00
b.	Refunds, rebates, etc.			
c.	Program income used in accordance with the deduction alternative			
d.	Net outlays (Line a, less the sum of lines b and c)	0.00	770,000.00	770,000.00
	Recipient's share of net outlays, consisting of:			
e.	Third party (in-kind) contributions			
f.	Other Federal awards authorized to be used to match this award			
g.	Program income used in accordance with the matching or cost sharing alternative			
h.	All other recipient outlays not shown on lines e, f or g			
i.	Total recipient share of net outlays (Sum of lines e, f, g and h)	0.00	0.00	0.00
j.	Federal share of net outlays (line d less line i)	0.00	770,000.00	770,000.00
k.	Total unliquidated obligations			
l.	Recipient's share of unliquidated obligations			
m.	Federal share of unliquidated obligations			
n.	Total Federal share (sum of lines j and m)			770,000.00
o.	Total Federal funds authorized for this funding period			770,000.00
p.	Unobligated balance of Federal funds (Line o minus line n)			0.00
	Program Income, consisting of:			
q.	Disbursed program income shown on lines c and/or g above			
r.	Disbursed program income using the addition alternative			
s.	Undisbursed program income			
t.	Total program income realized (Sum of lines q, r and s)			0.00

11. Indirect Expense

a. Type of Rate (Place "X" in appropriate box)	b. Rate	c. Base	d. Total Amount	e. Federal Share
☐ Provisional ☐ Predetermined ☐ Final ☒ Fixed	38.5%	125,706.40	48,396.98	48,396.98

12. Remarks: Attach any explanations deemed necessary or information required by Federal sponsoring agency in compliance with governing legislation.

This is a revised final report to include an Fisher Scientific invoice which was expended during the grant but not paid until after the ending date. Expense reimbursement approved by Bill Kokal DOE Chicago.

13. Certification: I certify to the best of my knowledge and belief that this report is correct and complete and that all outlays and unliquidated obligations are for the purposes set forth in the award documents.

Signature of Authorized Certifying Official	Telephone (Area code, number and extension) (308) 865-8524
Typed or Printed Name and Title Larry Riessland, Director of Finance	Date Report Submitted September 29, 2008

Previous Edition Usable
NSN 7540-01-012-4285

269-104
200-498 P.O. 139 (Face)

Standard Form 269 (Rev. 7-97)
Prescribed by OMB Circulars A-102 and A-110

Revenue Elements	Plan	Period 4	Year to Date	Life to Date	Commitments	$ Variance	% Uncoll.
461000 Plan Fed Grts&Cnts	770,000.00-	0	0	0.00	0	770,000.00-	100
461200 Federal Aid Payments	0	0.00	26,792.64-	770,000.00-	0	770,000.00	0
* Federal Grants & Contracts	770,000.00-	0.00	26,792.64-	770,000.00-	0	0.00	0
464400 Receivable Revenue	0	0.00	175.26	0.00	0	0.00	0
* Private Grants & Contracts	0	0.00	175.26	0.00	0	0.00	0
** Total Gifts, Grants, Contracts	770,000.00-	0.00	26,617.38-	770,000.00-	0	0.00	0
*** Total Revenue	770,000.00-	0.00	26,617.38-	770,000.00-	0	0.00	0

Cost Elements	Plan	Period 4	Year to Date	Life to Date	Commitments	$ Variance	% Remain
511000 Planned Faculty Salaries	53,578.00	0	0	0.00	0.00	53,578.00	100
511100 Faculty - Permanent	0	0	0	53,578.53	0	53,578.53-	0
* Faculty Salaries	53,578.00	0	0	53,578.53	0.00	0.53-	0-
513000 Plan Mgr/Prof Salary	40,000.00	0	0	0.00	0.00	40,000.00	100
513200 Mgr/Profess-Temp	0	0	0	40,000.00	0	40,000.00-	0
* Managerial/Professional	40,000.00	0	0	40,000.00	0.00	0.00	0
516000 Planned Student Wages	9,000.00	0	0	0.00	0.00	9,000.00	100
516500 Student Hourly	0	0	0	8,979.54	0	8,979.54-	0
* Student Wages	9,000.00	0	0	8,979.54	0.00	20.46	0
517000 Plan Other Per Svrs	8,444.00	0	0	0.00	0.00	8,444.00	100
517200 Other-Temporary	0	0	0	7,500.40	0	7,500.40-	0
* Other Salaries/Wages/Personal Servi	8,444.00	0	0	7,500.40	0.00	943.60	11
** Total Salaries & Wages	111,022.00	0	0	110,058.47	0.00	963.53	1
519000 Planned Benefits	15,693.00	0	0	0.00	0.00	15,693.00	100
* Planned Benefits	15,693.00	0	0	0.00	0.00	15,693.00	100
519100 Retirement Contribution	0	0	0	3,878.77	0	3,878.77-	0
* Retirement Contribution	0	0	0	3,878.77	0	3,878.77-	0
519200 FICA Contribution	0	0	0	4,296.81	0	4,296.81-	0
* FICA Contribution	0	0	0	4,296.81	0	4,296.81-	0
519300 Health Ins Contribut	0	0	0	7,428.05	0	7,428.05-	0
* Health Insurance Contribution	0	0	0	7,428.05	0	7,428.05-	0
519400 Life Insurance Contribution	0	0	0	44.30	0	44.30-	0
* Life Insurance Contribution	0	0	0	44.30	0	44.30-	0
** Total Benefits	15,693.00	0	0	15,647.93	0.00	45.07	0
*** Total Personal Services	126,715.00	0	0	125,706.40	0.00	1,008.60	1
520000 Plan Tot Operate Exp	400,468.00	0	0	0.00	0	400,468.00	100
521100 Postage	0	0	0	8.37	0	8.37-	0
521300 Freight and Cartage	0	0	0	22.88	0	22.88-	0
521302 Federal Express	0	0	0	170.19	0	170.19-	0
521500 Publish/Print/&Photo	0	0	0	306.00	0	306.00-	0
521800 Dues/Subscriptions/Fees	0	0	0	105.00	0	105.00-	0
521900 Conference Expense	0	0	0	4,416.00	0	4,416.00-	0
521950 Subsistence	0	0	0	928.75	0	928.75-	0
525900 R & M Other Equipment	0	0.00	22,798.00	22,798.00	0	22,798.00-	0
526001 Con Serv-Travel Exp	0	0	0	1,471.84	0	1,471.84-	0

		Plan	Period 4	Year to Date	Life to Date	Commitments	$ Variance	% Var
	526004 Subcontract Payments	0	0	0	384,933.00	0	384,933.00-	0
	526700 Laboratory Fees	0	0	0	270.00	0	270.00-	0
*	Operating Expenses/Services	400,468.00	0.00	22,798.00	415,430.03	0	14,962.03-	4-
	530000 Plan Sup & Materials	50,092.00	0	0	0.00	0	50,092.00	100
	531802 Shop Supplies	0	0	0	117.50	0	117.50-	0
	531996 Computing Supplies	0	0	0	136.95	0	136.95-	0
	533100 Research and Lab Supplies	0	0	0	44,313.89	0.00	44,313.89-	0
*	Operating Supplies	50,092.00	0	0	44,568.34	0.00	5,523.66	11
**	Total Operating & Supplies	450,560.00	0.00	22,798.00	459,998.37	0.00	9,438.37-	2-
	540000 Planned Travel Expenses	13,751.00	0	0	0.00	0	13,751.00	100
	541110 Lodging	0	0	0	2,696.30	0	2,696.30-	0
	541120 Meals	0	0	0	1,128.47	0	1,128.47-	0
	541200 Commercial Fares	0	0	0	62.30	0	62.30-	0
	541201 Comm Fares-Desig Age	0	0	0	2,000.50	0	2,000.50-	0
	541300 University/State Fares	0	0	0	463.78	0	463.78-	0
	541400 Mileage Allowance	0	0	0	568.78	0	568.78-	0
	541500 Misc Travel Expense	0	0	0	44.50	0	44.50-	0
*	Domestic Travel Expense	13,751.00	0	0	6,964.63	0	6,786.37	49
**	All Travel Domestic and Foreign	13,751.00	0	0	6,964.63	0	6,786.37	49
	550000 Planned Capital Expenses	130,313.00	0	0	0.00	0	130,313.00	100
	553270 Cap Eq-Ed&Recreation	0	0.00	3,819.38	109,821.88	0.00	109,821.88-	0
	553800 Capital Research Equipment	0	0	0	19,111.74	0	19,111.74-	0
**	Capital Outlay	130,313.00	0.00	3,819.38	128,933.62	0.00	1,379.38	1
***	Total Non-Personal Services	594,624.00	0.00	26,617.38	595,896.62	0.00	1,272.62-	0-
****	Total Direct Costs	721,339.00	0.00	26,617.38	721,603.02	0.00	264.02-	0-
	580000 Plan Indir Cost & Ot	48,661.00	0	0	0.00	0	48,661.00	100
	581000 Indirect Cost Charges	0	0	0	48,396.98	0	48,396.98-	0
****	Other Deductions	48,661.00	0	0	48,396.98	0	264.02	1
*****	Total Expense	770,000.00	0.00	26,617.38	770,000.00	0.00	0.00	0

Revenue (over)/under expense	Plan	Period 4	Year to Date	Life to Date	Commitments	$ Variance	% Var.
Revenue (over)/under expense	0.00	0.00	0.00	0.00	0.00	0.00	0

*****COMMITMENTS REFLECT ALL OPEN ITEMS AS OF 10/01/2008.

Copper-Indium-Boron-Diselenide Absorber Materials

Natale J. Ianno[1], Rodney J. Soukup[1], Tobin Santero[1], Chad Kamler[1], James Huguenin-Love[1], Scott A. Darveau[2], Jiri Olejnicek[2], and Christopher L. Exstrom[2]

[1]Dept. of Elec. Eng., University of Nebraska-Lincoln, 209N WSEC, Lincoln, NE, 68588-0511

[2]Dept. of Chemistry, University of Nebraska at Kearney, 905 West 25th Street, Kearney, NE, 68849-1150

ABSTRACT

Attempts to fabricate new $CuIn_{1-x}B_xSe_2$ (CIBS) and $CuBSe_2$ (CBS) thin-film materials have been complicated by the formation of interfering crystallites and by the loss of boron from the magnetron sputtered precursor alloys during the selenization and annealing processes. Raman and Auger spectroscopic analysis as well as X-ray diffraction studies show that the formation of boron selenide may be contributing to the difficulty in creating these new materials.

INTRODUCTION

While much progress has been made in photovoltaic cell development, the United States still does not have a cost-competitive version of a solar cell for domestic or industrial applications except in very remote areas of the country. In order for photovoltaic systems to be competitive, a 15% module efficiency with an installed efficiency of 12% at a cost of $1/Wp and a 20 year lifetime must be achieved. Broad-based U.S. government-supported research has determined that this goal can most likely be met by thin-film solar cells [1]. Of these thin film materials, the $CuInSe_2$ (CIS) family shows the most promise [2]. Unfortunately, solar cells produced with CIS as the absorber layer are limited in efficiency as a consequence of the relatively small bandgap of 1.04 eV [3]. Ongoing research has been directed toward materials for which lighter elements from group IIIA of the periodic table are substituted in part for the indium in order to increase the bandgap.

To date, the greatest energy conversion efficiency, 19.5%, has been achieved with a $CuIn_{0.74}Ga_{0.26}Se_2$ (CIGS) absorber layer which has a bandgap of 1.15 eV with an open circuit output voltage of 0.701 V [4,5]. Changes in the bandgap structure limits the maximum amount of Ga that can be substituted and still allow the solar cell to maintain this higher efficiency.

We are working toward the fabrication and study of a new material, copper indium boron diselenide, $CuIn_{1-x}B_xSe_2$ (CIBS), which, to the best of our knowledge, has never been grown and studied. Boron should yield a higher bandgap, closer to the ideal value of 1.5 eV, for lower concentrations of boron than either gallium or aluminum [6]. We anticipate this lower concentration to lead to thin ordered films approaching the idealized chalcopyrite crystal structure of CIS. This material has not been studied because the excessively high boiling point of boron prevents its deposition by evaporation, the classical means of producing CIS-based solar cell films.

Boron concentration in the films is a critical parameter in projecting what bandgaps may be achieved. Based on the results for Ga and Al substitution, [6] we have calculated that less than 24% boron will result in a bandgap near 1.5 eV. To estimate this, the bandgaps of $CuInSe_2$, $CuGaSe_2$, and $CuAlSe_2$ were plotted as a function of the atomic mass of the column III elements

and a perfect logarithmic fit was found, see figure 1. This curve was then extrapolated to the atomic mass of B and yielded an estimated bandgap for $CuBSe_2$ of $E_g = 3.16eV$. Equation (1) in the paper by Wei and Zunger [6] is repeated here

$$E_g(x) = (1-x)\,E_g(A) + x\,E_g(B) - bx(1-x) \qquad (1)$$

where A is indium and, in our case, B is boron and x is the fraction of boron concentration. This equation was then used to determine x, the fraction of B to be used. Given that reported b values for Cu(Al,Ga)Se_2 and Cu(Ga,In)Se_2 range from -0.07 to 0.28[6], b values between -0.1 and 0.4 were applied in our calculation to yield an x value range of 21-25 at. % for a CIBS film to have a bandgap near 1.5 eV. Thus, the concentration required to achieve a given band gap is not strongly dependent on the parameter b. This percentage is comparable to the Ga-substitution percentage in CIGS which yields the highest efficiency solar cell to date [3]. Thus, it appears feasible that a CIBS film with chalcopyrite structure integrity can be fabricated.
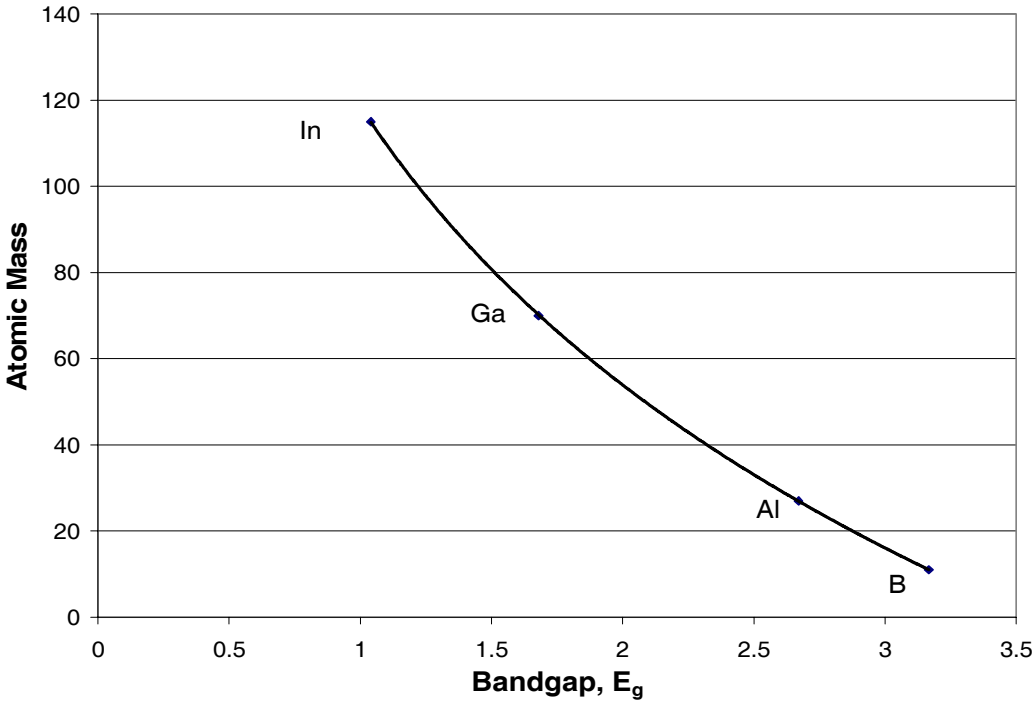
Figure 1. Approximate bandgaps of CuXSe$_2$ (X = B, Al, Ga, In) as a function of the atomic mass of X. Values for CuAlSe$_2$, CuGaSe$_2$, and CuInSe$_2$ bandgaps are from ref. 6. The trend is extrapolated to estimate the CuBSe$_2$ bandgap.

EXPERIMENT

The copper-indium and copper-indium-boron precursor films were co-sputtered in an AJA International ATC 1600 Sputtering System that routinely reaches a base pressure of approximately 1×10^{-4} Pascal. The argon sputtering gas is directly injected between the target and ground shield of each planar magnetron sputter gun, at a flow rate of 15 sccm into each gun. The

substrates were loaded into the chamber through a load lock onto the rotating, heated substrate holder.

The copper and indium guns were driven by dc power supplies, while the boron gun was driven by an rf supply. The precursor samples, all between 400 and 600nm thick, were analyzed by Auger Depth Profiling to determine their composition and uniformity. All samples were selenized in a quartz halogen lamp heating system using a solid, pure selenium source. The selenium was placed in a graphite boat along with the substrate. The boat was loaded into a quartz tube which was evacuated by a mechanical pump to a base pressure of less than 1 Pascal. A thermocouple is embedded into the boat and serves as the process temperature monitor. A two step ramp and soak process was employed where a 10 minute ramp to 250 $^{\circ}$C followed by a 20 minute soak were followed by another 10 minute ramp to the selenization temperature and another 20 minute soak. A controlled cool down returned the boat to room temperature [7].

Selenized samples were characterized by θ-2θ X-ray diffractometry, Raman Spectroscopy and Auger Depth Profiling.

RESULTS AND DISCUSSION

A comparison of XRD spectra for precursor Cu_xIn_y, $Cu_{x'}In_{y'}B_{z'}$ and $Cu_{x''}B_{z''}$ films showed that boron had virtually no effect on the observed Cu_2In and Cu_9In_{11} peaks. The XRD spectra for the selenized precursors are seen in figure 2. Peaks consistent with CIS-type structure are apparent for both selenized Cu_xIn_y and $Cu_{x'}In_{y'}B_{z'}$ films. Results from the selenized $Cu_{x''}B_{z''}$ film are most consistent with several $Cu_{2-x}Se$ phases.
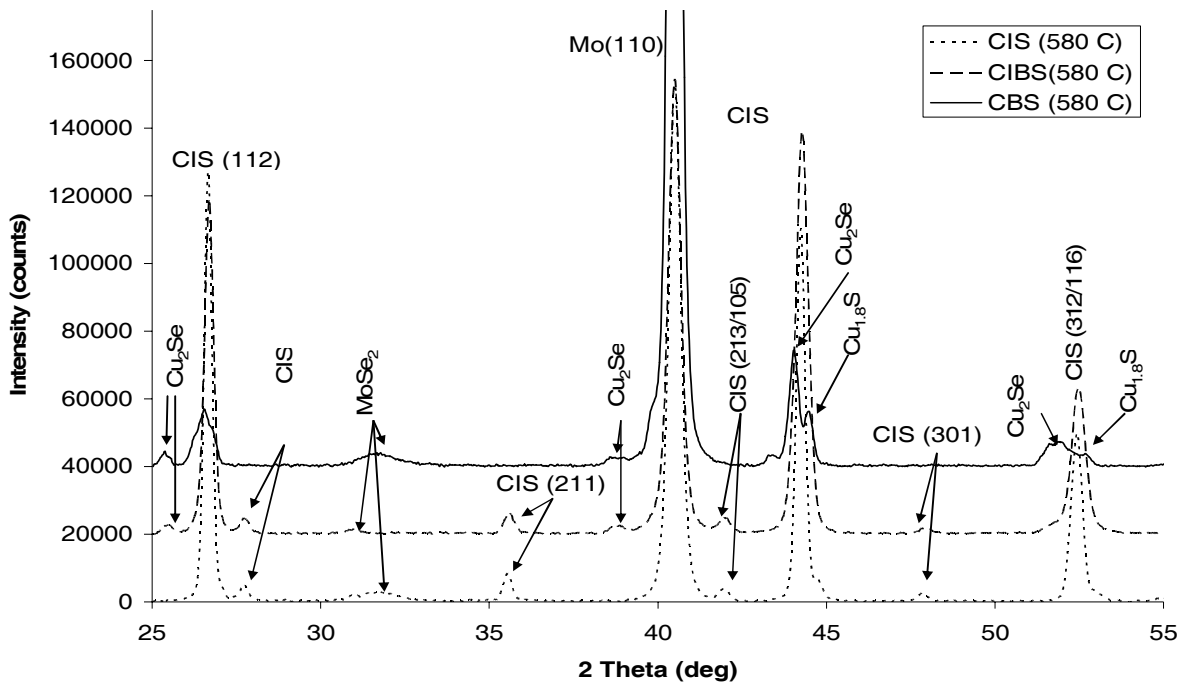
Figure 2. X-ray diffraction scans of CIS, CIBS and CBS films. The intensity of the CIBS and CBS films are offset for clarity.

The expected shift in the CIS (112) peak for the selenized $Cu_{x'}In_{y'}B_{z'}$ film as a result of substituting the smaller boron atom for the indium is not apparent and any small shift may be more consistent with mixed CIS and $Cu_{1.8}Se$ phases [8-10].

Raman Spectra of the same Cu_xIn_y, $Cu_{x'}In_{y'}B_{z'}$ and $Cu_{x''}B_{z''}$ films following selenization at 580^oC are seen in figure 3. Note the presence of $CuInSe_2$ signals from the selenized Cu_xIn_y and $Cu_{x'}In_{y'}B_{z'}$ films and the lack of a signal near 170 - 190 cm^{-1} for the selenized $Cu_{x''}B_{z''}$ film.
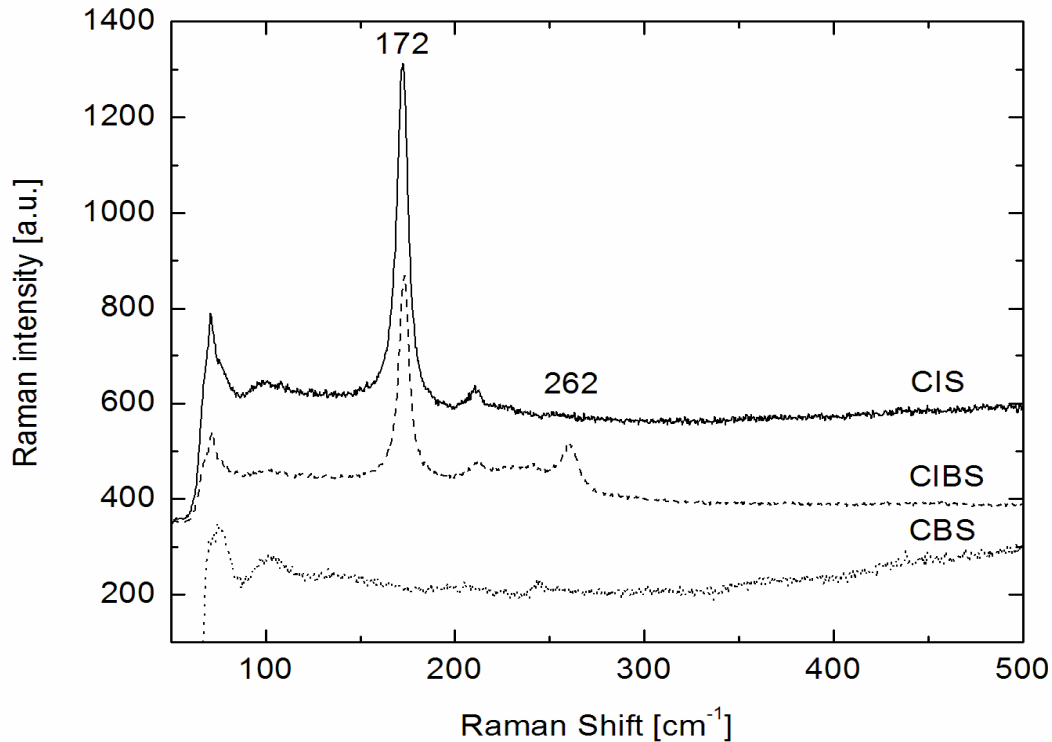
Figure 3. Raman spectrum of Cu_xIn_y, $Cu_{x'}In_{y'}B_{z'}$ and $Cu_{x''}B_{z''}$ films following selenization at 580^oC

Optical microscope images of selenized $Cu_{x'}In_{y'}B_{z'}$ films revealed isolated surface crystallites with apparently distinct morphologies. When the incident laser beam was focused on these crystallites, the Raman spectra seen in Fig. 4 included a peak near 840 cm^{-1} that is consistent with the presence of B_2Se_3 [11]. Portions of the films outside these crystallites gave Raman spectra with no peak at 840 cm^{-1} but otherwise identical to figure 4. The resulting conclusion is that B remains in the film in isolated regions, rather than throughout the entire film.

Figure 5 shows an Auger depth profile of a selenized $Cu_{x'}In_{y'}B_{z'}$ film. An Auger depth profile was run on the film prior to selenization. The results indicated that copper, indium and boron were uniform throughout the film. Sputter deposition of this film was accomplished using a 45%Cu-55%In target, a second pure Cu target and a B target. The precursor film contained about 57% copper, 28% boron and 15% indium. A look at the analysis presented in figure 5 illustrates that the elements are no longer uniformly distributed after selenization, but that the boron accumulates at the bottom of the film while copper and selenium decrease in relative

concentration as a function of depth into the film. The indium signal appears to peak near the center of the film. In order to confirm that this was not a result of the selenization process, numerous copper indium precursors selenized and depth profiled and showed uniform distribution of the elements through the thickness of the film.
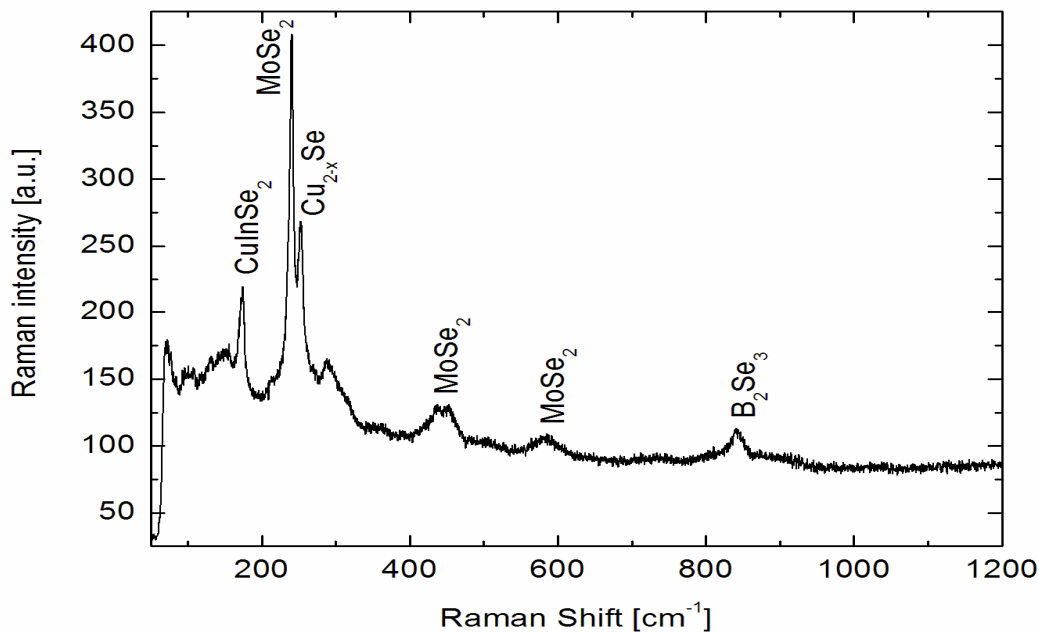
Figure 4. Raman Spectra of a crystallite on the surface of a selenized copper-indium-boron film and the surrounding area.
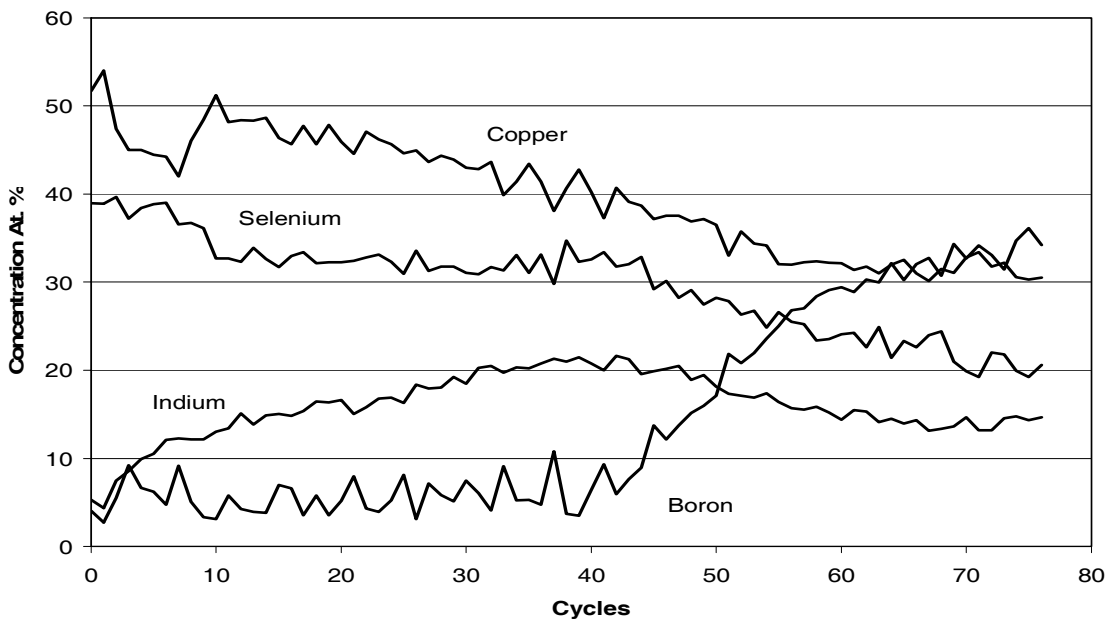
Figure 5. Auger depth profile of a selenized copper-indium-boron film.

CONCLUSIONS

The magnetron sputtering system is capable of introducing boron into a CuIn metal alloy. However, the selenization and annealing processes appear to result in either the loss of boron entirely or the formation of an undesirable B_2Se_3 phase atop a $CuInSe_2$ or $Cu_{2-x}Se$ layer. The remaining boron appears to accumulate near the film-substrate interface. A similar result for aluminum was observed for selenized $CuIn_{1-x}Al_x$ precursors.[12]

Future experiments are needed in order to optimize the selenization and annealing processes to overcome the boron selenide formation, boron loss, and boron segregation problem. One potential approach may be to allow the formation of the boron selenide followed by the deposition of a Cu(In) overlayer that upon annealing may trap the boron and force the formation of $CuIn_{1-x}B_xSe_2$ or $CuBSe_2$. These new experiments are being carried out.

ACKNOWLEDGMENTS

REFERENCES

1. R.J. Soukup, Jemná Mechanika a Optika **1**, 12 (1995).
2. R. Noufi, K. Zweibel in *Proceedings 2006 IEEE 4th World Conference on Photovoltaic Energy Conversion*, (Institute of Electrical and Electronics Engineers, Inc. (IEEE) Vol. 1: Piscataway, NJ 2006) pp. 317-320.
3. K. Ramanathan, G. Teeter, J.C. Keane and R. Noufi, Thin Solid Films **480-481**, 499 (2005).
4. M.A. Contreras, K. Ramanathan, J. AbuShama, F. Hasoon, D.L. Young, B. Egaas and R. Noufi, Progress in Photovoltaics: Research and Applications **13**, 209 (2005).
5. J.T. Heath, J.D. Cohen and W.N. Shafarman in *Compound Semiconductor Photovoltaics*, edited by R.Noufi, W. N. Shafarman, D. Cahen, and L. Stolt, (Mat. Res. Soc. Symp. Proc. **763** Pittsburgh, PA, 2003) pp. B9.2.1-B9.2.6.
6. S.-H. Wei and A. Zunger, J. Appl. Phys. **78**, 3846 (1995).
7. F. Adurodija, J. Song, S.K. Kim, Ki.H.Kang, K.H. Yoon, S.H. Kwon, B.T. Ahn, and S.D. Kim, Journal of the Korean Physical Society **32**, 87 (1998).
8. W. Gebicki , M. Igalson , W. Zajac, and R. Trykozko, Journal of Physics D: Applied Physics **23**, 964 (1990).
9. Y.B.K. Reddy, V.S. Raja, and B. Sreedhar, Journal of Physics D: Applied Physics **39**, 5124 (2006).
10. D.K. Suri, K.C. Nagpal, and G.K. Chadha, Journal of Applied Crystallography **22**, 578 (1989).
11. R. Hillel, and J. Cueilleron, Bulletin De Laq Société Chemique de France **1**, 98, (1972).
12. J.H. Yun, R.B.V. Chalapathy, J.C. Lee, J. Song, and K.H. Yoon, Solid State Phenomena **124-126**, 975 (2007).

REACTION PATHWAY INSIGHTS INTO THE SOLVOTHERMAL PREPARATION OF $CuIn_{1-x}Ga_xSe_2$ NANOCRYSTALLINE MATERIALS

Christopher L. Exstrom, Scott A. Darveau, Andrea L. Martinez-Skinner, Matt Ingersoll, Jiri Olejnicek, Anatole Mirasano, and Adam T. Haussler
Department of Chemistry, University of Nebraska at Kearney, Kearney, NE 68849-1150

James Huguenin-Love, Chad Kamler, Martin Diaz, N. J. Ianno, and R. J. Soukup
Department of Electrical Engineering, University of Nebraska-Lincoln, Lincoln, NE 68588-0511

ABSTRACT

Reaction pathway investigations of the solvothermal preparation of nanocrystalline $CuIn_{1-x}Ga_xSe_2$ in triethylenetetramine reveal the early formation of a previously unreported $Cu_{2-x}Se(s)$ intermediate. Over 24 hours, this reacts with In and Se species to form $CuInSe_2(s)$. If Ga is present, the reaction proceeds over an additional 48 hours to form $CuIn_{1-x}Ga_xSe_2$. Adding ammonium halide salts reduces the $CuInSe_2$ formation time to as little as 30 minutes. It is proposed that in these cases, $Cu_{2-x}Se$ particle growth is limited via a competitive Cu-halide complex formation. The smaller $Cu_{2-x}Se$ particles may react and form $CuInSe_2$ more rapidly. A reaction pathway scheme consistent with experimental results and previous literature reports is proposed.

INTRODUCTION

For some time, the chalcopyrite semiconductors $CuInSe_2$ (CIS) and $CuIn_{1-x}Ga_xSe_2$ (CIGS) have been leading thin-film material candidates for incorporation in high-efficiency photovoltaic devices [1-4]. Interest in the development of more cost-effective, non-vacuum film production techniques has stimulated research in the solution-based preparation of nanocrystalline CIS and CIGS. Reported nanocrystal preparations involve solvothermal processes in which constituent elements or their salts are heated in a solvent. While a variety of reaction conditions have successfully yielded nanocrystalline CIS [5-10], and to a lesser extent CIGS [11, 12], no systematic study of the solvothermal reaction mechanism(s) or structure-activity relationships has been conducted. A better mechanistic understanding of this solvothermal preparation may lend insight into the synthesis of new $CuIn_{1-x}M_xSe_2$ (M = Ga, Al, B) chalcopyrite materials.

Most early reported procedures for solvothermal CIS and CIGS formation involved superheating a sealed container of Cu, In, Ga, and Se sources in ethylenediamine (en) solvent at 140-280 °C for 15-36 hours [5-8]. The reaction directly yields nanocrystals. Proposed mechanisms for these solvothermal processes involve the formation of separate indium and gallium selenide species that react with a solvated Cu^+ complex to form CIS or CIGS. Following initial Cu^{2+} and Se reduction, CIS formation is proposed to occur as follows [9, 12]:

$$2 InCl_3 + 3 Se^{2-} \rightarrow In_2Se_3 + 6 Cl^- \qquad (1)$$
$$In_2Se_3 + Se^{2-} \rightarrow 2 InSe_2^- \qquad (2)$$
$$InSe_2^- + [Cu(en)_2]^+ \rightarrow CuInSe_2 + 2 en \qquad (3)$$
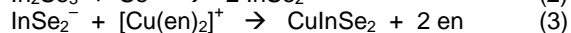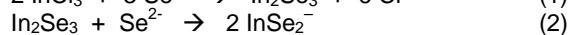
In the formation of CIGS isometric nanoparticles, it has been proposed that $[Cu(en)_2]^+$ reacts with separately-formed In_2Se_3 and Ga_2Se_3 phases [12]. While reported mechanism proposals are consistent with the CIS and CIGS solvothermal preparations, there has been no experimental evidence of any of the proposed intermediates.

Solvent selection is proving to be important in the engineering of CIS and CIGS nanocrystal size and morphology. Early attention focused on en because of possibilities that the square-planar geometry of the $[Cu(en)_2]^+$ intermediate complex would promote one-dimensional nanorod growth [9]. More recent reports [10, 13] describe the use of surfactant-based phosphine and amine solvents such as trioctylphosphine (TOP), tributylphosphine (TBP), octadecylamine, and oleylamine in order to control the growth rate of newly formed nanocrystals. Generally, the bulk of the solvent molecules and the size of stabilized nanoparticles are inversely related [14]. Stabilization of small nanoparticles seems to be related to formation reaction rate. Using these surfactant-based solvents, CIS and CIGS formation reaction times of 30-60 minutes have been reported [13].

An advantage of using en and chemically similar solvents that coordinate strongly to transition metals in molecular complexes is that reaction intermediates may be better shielded from oxidation in open-air syntheses. We have recently demonstrated the first open-air solvothermal preparation of nanocrystalline $CuIn_{1-x}Ga_xSe_2$ of wide-ranging Ga/In ratios (x = 0, 0.21, 0.35, 0.79, 1) [15]. At all compositions, morphologies consist of a mixture of isometric nanocrystalline growths (10-40 nm diameters), larger plates (50-100 nm diameters) and nanorods (see Fig. 1).
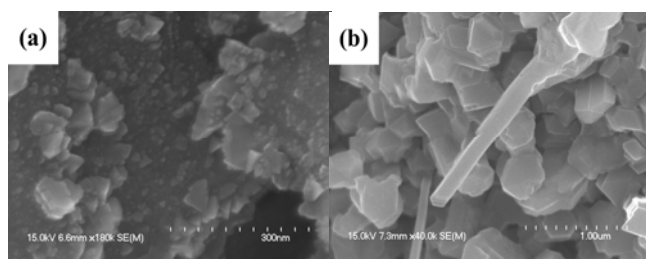
Fig. 1. SEM images of (a) $CuIn_{0.79}Ga_{0.21}Se_2$ and (b) $CuGaSe_2$ nanocrystals prepared solvothermally [15].

Fig. 2. Molecular structures of (a) ethylenediamine and (b) triethylenetetramine

In this paper, we report studies of the solvothermal reaction pathway in triethylenetetramine (trien). This solvent is chemically similar to en (see Fig. 2) but has a higher boiling point (267 ^{o}C) that appears to be necessary to incorporate Ga in the chalcopyrite crystalline lattice and form CIGS [12]. In the CIS preparation, the initial formation of a previously unreported $Cu_{2-x}Se$ solid-state intermediate is observed. Over time, this compound reacts with Se and one or more In species to form CIS. If Ga is present, conversion to CIGS proceeds. The reaction rate is accelerated by the presence of soluble ammonium and halide salts in the reaction mixture. A reaction pathway scheme that is consistent with our results and previous literature is proposed.

EXPERIMENTAL

Desired stoichiometric quantities of $CuCl_2$, $InCl_3$, $GaCl_3$, and Se were combined in triethylenetetramine (trien) solvent and refluxed with stirring for times ranging from five minutes to 48 hours. The reaction mixture was cooled to room temperature and centrifuged. Following the decanting of the solvent, the remaining black solid was washed with methanol and deposited onto a glass or Mo-glass substrate via spin coating from a methanol/CH_2Cl_2 suspension. Products were characterized by micro-
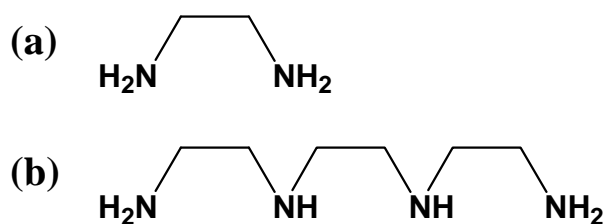
Raman spectroscopy, Auger electron spectroscopy (AES), X-ray diffraction (XRD), and scanning electron microscopy (SEM). In reaction rate acceleration investigations, the reaction mixture included a 2- to 18-mole excess (relative to Cu) of NH_4Cl or other salt in the reaction mixture.

RESULTS AND DISCUSSION

Solvothermal Reaction Pathway for CIS and CIGS Formation

We have gained information about the CIS preparation reaction pathway in trien solvent from the analysis of stable solid-state intermediates. Upon combining stoichiometric quantities of $CuCl_2$, $InCl_3$, and Se in trien, Raman peak(s) for $Cu_{2-x}Se$ (~ 255 cm^{-1}) [16] are observable within five minutes. At this point, Se (~ 235 cm^{-1}) [17] and $Cu_{2-x}Se$ solids are observable by Raman spectroscopy (Fig. 3a). From XRD spectroscopy, this $Cu_{2-x}Se$ phase is identified as berzelianite ($Cu_{1.8}Se$), the same composition that was use to model copper-deficient Cu_2Se XRD signal phase fitting in *in-situ* XRD studies of solid-state CIGS formation reactions [18].

No Se XRD signals appear, indicating that at this point, the Se in the sample is amorphous. As the reaction
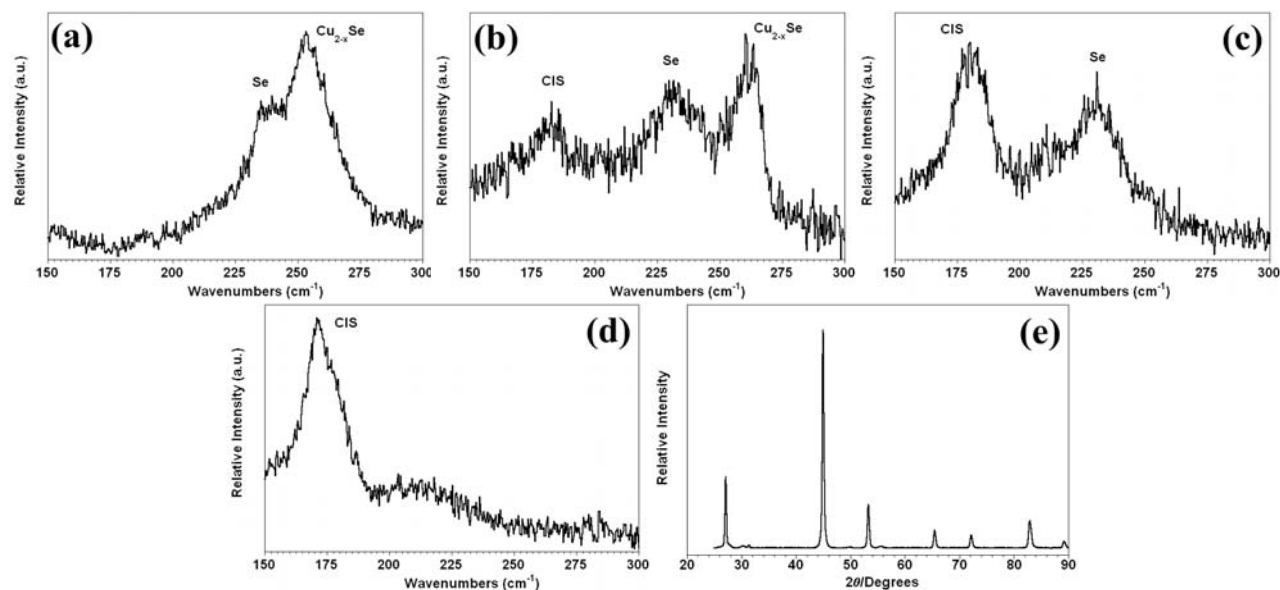

Fig. 3. Raman spectra of solid products from reaction between $CuCl_2$, $InCl_3$, and Se in refluxing trien after reactions times of (a) 5 min, (b) 1 hr, (c) 6 hr, and (d) 24 hr reaction times. (e) XRD pattern of same material as in (d).

progresses, a CIS Raman peak (~ 170 cm^{-1}) [19] starts to grow in after 1 hour (Fig. 3b). As CIS forms, the $Cu_{1.8}Se$ peak disappears within six hours (Fig. 3c). After 24 hours, all Se has been reacted (Fig. 3d), and the XRD spectrum shows only CIS (Fig. 3e).

Neither Raman spectroscopy nor XRD indicate the presence of any solid-state In species. This lends support to the formation of $InSe_2^-$ as in (2) or a solvated complex such as $[In(trien)_x]^{3+}$, as amines are known to coordinate to In^{3+} as labile ligands [20]. Nuclear magnetic resonance (NMR), electrochemical, and spectroscopic studies of soluble reaction species are in progress.

Studies of CIGS solvothermal formation indicate that the reaction initially proceeds to CIS as described above (Figs. 3a-d) followed by a slow reaction with one or more soluble Ga species to form CIGS. This is consistent with reported $[Ga(amine)_x]^{3+}$ formation constants that are two orders of magnitude larger than those for analogous $[In(amine)_x]^{3+}$ complexes [20]. In reported solid-state mechanisms, separately-crystallized CIS and CGS interdiffuse to form CIGS [21]. From solvothermal reaction products, we have seen no evidence of simultaneously present CIS and CGS Raman and XRD signals.

The formation of $Cu_{2-x}Se(s)$ is absent from previously proposed solvothermal mechanisms and raises questions about the stability of $[Cu(amine)_x]^+$ complexes in this reaction pathway. While metal-solvent complexes may be important intermediates in the reduction of Cu and the fast formation of $Cu_{2-x}Se(s)$, it is more likely that this solid-state species is the immediate precursor to CIS.

Reaction Acceleration Effects of Added Ionic Salts

The role of specific starting material counterions or solution ionic strength in solvothermal CIS preparations has not been investigated. Given that solution-phase charged complexes may be important in solvothermal preparation mechanisms, it is feasible that solution ionic strength or counterion presence could affect the stability of these complexes during the reaction. The reported process for electrodeless deposition of CIGS from aqueous solution employs a 10-fold excess of LiCl as a "background electrolyte" [22]. Most likely, this facilitates the various redox reaction steps involved in the CIGS deposition.

$CuCl_2$, $InCl_3$, and Se were reacted in refluxing trien solvent that contained a 2- to 18-times mole excess (relative to Cu) of an ammonium or halide salt. Reaction rates are greatly accelerated. Pure CIS (as determined by Raman and XRD spectroscopy) can be prepared in as little as 30 minutes when an 18-fold NH_4Cl excess is present. This compares to 24 hours without any NH_4Cl in the reaction mixture. Tables 1 and 2 summarize the CIS reaction completion times when various salts are present in the reaction mixture.

Table 1. Solvothermal CIS Formation Times, in Hours, with added Ammonium Salts

equiv present[a]	NH_4Cl	NH_4Br	NH_4I	NH_4PF_6
0	24	24	24	24
2	6	8	14	24
6	1	4	6	24
18	0.5	1	2	24

[a]molar equivalents relative to Cu

CIS formation times vary with the nature of halide ion (Cl-, Br-, I-) in the added ammonium salt. Halide ions are known to form complexes with Cu^+ and In^{3+} [23, 24], and the reaction times correlate inversely with the relative stabilities of $[Cu(amine)_3X]$ (X = Cl-, Br-, I-) complex formation [25]. The presence of PF_6^-, a non-coordinating anion, does not accelerate the reaction. This supports the idea of Cu- and/or In-halide complex formation in the reaction pathway.

Table 2. Solvothermal CIS Formation Times, in Hours, with added Chloride Salts

equiv present[a]	NH_4Cl	$(CH_3)_4NCl$	$CaCl_2$
0	24	24	24
2	6	14	n.d.[b]
6	1	6	n.d.
18	0.5	2	12

[a]molar equivalents relative to Cu
[b]not determined

CIS formation times also vary with the nature of the cation in the added salt. Effects of NH_4^+ and $(CH_3)_4N^+$ may be directly compared. It is unlikely that the greater rate acceleration effect of NH_4^+ is due to proton transfer to trien followed by NH_3 complexation to Cu or In, as NH_3 is less basic ($pK_b = 4.75$) [26] than trien ($pK_b = 3.21$) [27]. It is possible that with its larger charge density (smaller ion size), NH_4^+ may better stabilize a negatively-charged Cu- and/or In-halide complex in the reaction pathway. This would imply that the presence of smaller inorganic cations may accelerate the reaction to a greater extent. Unfortunately, $CaCl_2$ was only slightly soluble in the reaction mixture, while $MgCl_2$, NaCl and KCl were insoluble.

Proposed Reaction Pathway Scheme

A modified CIS/CIGS solvothermal preparation reaction pathway scheme based on our experimental results and previously reported literature is proposed in Figure 4.
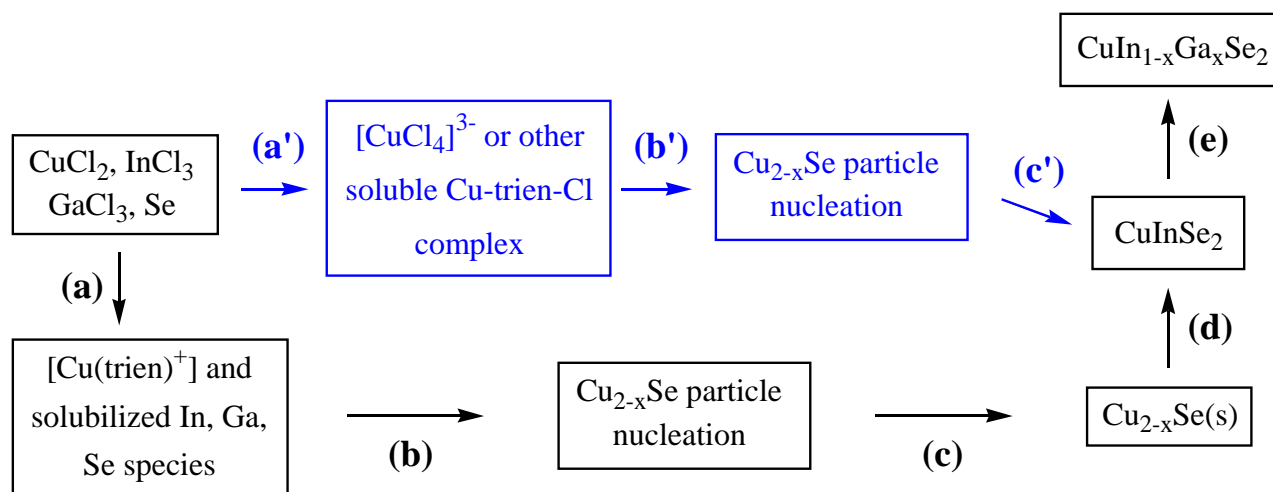
Fig. 4. Proposed reaction pathway scheme for the solvothermal preparation of nanocrystalline $CuIn_{1-x}Ga_xSe_2$ in triethylenetetramine. See the text for descriptions of the lettered steps. The blue pathway steps (a'), (b'), and (c') are proposed to be adopted in place of steps (a) through (d) when NH_4Cl is present in the reaction mixture.

Step (a) – Solubilization of source elements. Upon combining $CuCl_2$, $InCl_3$, $GaCl_3$, and Se in trien, the solution immediately turns deep blue, indicative of $[Cu(trien)]^+$ formation. Se appears to slowly dissolve at room temperature. Amine solvents are known to activate and solubilize Se as $Se(amine)_x$ complexes [28]. Upon heating, $InCl_3$ and $GaCl_3$ dissolve, presumably as amine complexes, such as $[In(trien)]^{3+}$ and $[Ga(trien)]^{3+}$, and/or as selenide ions such as the previously proposed $InSe_2^-$ [9, 12]. No In or Ga species were observed in solid-state intermediates by Raman, XRD, or AES. This indicates that such intermediates remain in solution until the CIS formation step.

Step (b) – $Cu_{2-x}Se$ particle nucleation. Molecular clusters of $Cu_{2-x}Se$ form upon reaction of solvated Cu and Se species. The first black $Cu_{2-x}Se$ precipitate is observed with the reaction mixture reaches the trien boiling point (267 ^{o}C).

Step (c) – $Cu_{2-x}Se$ particle growth. In trien solvent under reflux conditions, this growth is expected to proceed rapidly. Without long carbon chains in their molecular structures, the trien molecules cannot stabilize [14] newly formed $Cu_{2-x}Se$ particles and prevent growth through addition of $Cu_{2-x}Se$ molecular clusters.

Steps (d) and (e) – CIS and CIGS formation. Over a period of 24 hours at reflux temperature, the solid $Cu_{2-x}Se$ reacts with solution-phase In to form CIS nanocrystals. If Ga is present, it will react with CIS over an additional 48 hours at reflux temperature to form CIGS.

Connection between Reaction Rates and Intermediate $Cu_{2-x}Se(s)$ Particles. Surfactant-based solvents have recently been reported to accelerate CIS and CIGS nanoparticle formation [13]. Although no explanation for this has been proposed, it is reasonable

that through increased accessible surface area, smaller $Cu_{2-x}Se$ particles would react with dissolved In faster than larger $Cu_{2-x}Se$ particles would react. Because surfactant-based solvents can stabilize nanoparticles at earlier stages in their growth, nanoparticle intermediates in CIS/CIGS solvothermal preparation reactions would react faster in surfactant-based solvents than in non-surfactants like en and trien.

Reaction Acceleration Effects of Added Salts. If the accelerated CIS formation reaction times in Tables 1 and 2 stem from the stabilization and subsequent reaction of smaller $Cu_{2-x}Se$ intermediate particles, the addition of ammonium halide salts would appear to have a "surfactant" effect on the reaction. Because the halide ions are negatively charged, it is not reasonable to propose that they stabilize newly-formed $Cu_{2-x}Se$ nanoparticles through a capping phenomenon. Considering our evidence of Cu-halide complex formation, the growth of $Cu_{2-x}Se$ particles may be inhibited by a competitive Cu-halide complex formation mechanism (steps (a') and (b') in Figure 4). This would result in an accelerated reaction (step (c') in Figure 4) of smaller intermediate $Cu_{2-x}Se$ particles with In.

CONCLUSION

Reaction pathway studies of the solvothermal preparation of nanocrystalline $CuIn_{1-x}Ga_xSe_2$ in triethylenetetramine have resulted in experimental evidence of a solid-state $Cu_{2-x}Se$ intermediate and reaction rate acceleration by added ammonium halide salts. The proposed reaction pathway scheme features solubilization of Cu, In, Ga, and Se starting materials, rapid nucleation and growth of $Cu_{2-x}Se(s)$ particles, and subsequent reactions of these with a soluble In species, forming CIS, followed by reaction with a soluble Ga species, forming CIGS. Halide anions from added

ammonium salts are believed to accelerate the reaction by limiting $Cu_{2-x}Se$ particle growth through a competitive Cu-halide complex formation step. The smaller $Cu_{2-x}Se$ particles may react faster with In to form CIS. Further experimental work, including microscopy of $Cu_{2-x}Se$(s) intermediates formed under different experimental conditions, investigation of surfactant-based solvent effects on reaction rate, and identification of soluble In and Ga intermediate species, to test the validity of this reaction scheme is underway.

REFERENCES

[1] A. Rockett and R.W. Birkmire, "Copper indium selenide ($CuInSe_2$) for photovoltaic applications" , *J. Appl. Phys.* **70**, 1991, pp. R81-R97.

[2] C. Guillen and J. Herrero, "Optical properties of electrochemically deposited copper indium selenide ($CuInSe_2$) thin films", *Solar Energy Mater.* **23**, 1991, pp. 31-45.

[3] U. Rau and H.W. Schock, "Electronic properties of $Cu(In,Ga)Se_2$ heterojunction solar cells. Recent achievements, current understanding, and future challenges", *Appl Phys. A: Mat. Sci. Process.* **69**, 1999, pp. 131-147.

[4] A. Miguel, K. Contreras, et. al., "Diode Characteristics in State-of-the-Art $ZnO/CdS/Cu(In_{1-x}Ga_x)Se_2$ Solar Cells", *Prog. Photovolt.: Res. Appl.* **13**, 2005, pp. 209-216.

[5] C.J. Carmalt, D.E. Morrison, and I.P.Parkin, "Solid-state and solution phase metathetical synthesis of copper indium chalcogenides", *J. Mater. Chem.* **8**, 1998, pp. 2209-2211.

[6] B. Li, Y. Xie, et. al., "Synthesis by a solvothermal route and characterization of $CuInSe_2$ nanowhiskers and nanoparticles", *Adv. Mater.* **11**, 1999, pp. 1456-1459.

[7] Y. Jiang, Y. Wu, et. al., "Elemental Solvothermal Reaction to Produce Ternary Semiconductor $CuInE_2$ (E = S, Se) Nanorods", *Inorg. Chem.* **39**, 2000, pp. 2964-2965.

[8] K.-H. Kim, Y.-G. Chun, et. al., "Synthesis of $CuInSe_2$ and $CuInGaSe_2$ nanoparticles by solvothermal route", *Mater. Sci. Forum* **449-452**, 2004, pp. 273-276,.

[9] Y.-H. Yang and Y.-T. Chen, "Solvothermal preparation and spectroscopic characterization of copper indium diselenide nanorods", *J. Phys. Chem. B* **110**, 2006, pp. 17370-17374.

[10] H. Zhong, Y. Li, et. al., "A facile route to synthesize chalcopyrite $CuInSe_2$ nanocrystals in non-coordinating solvent", *Nanotechnol.* **18**, 2007, pp. 025602 1-6.

[11] D.L. Schulz, C.J. Curtis, et. al., "Cu-In-Ga-Se nanoparticle colloids as spray deposition precursors for $Cu(In,Ga)Se_2$ solar cell materials", *J. Electron. Mater.* **27**, 1998, pp. 433-437.

[12] Y.-G. Chun, K.-H. Kim, and K.-H. Yoon, "Synthesis of $CuInGaSe_2$ nanoparticles by solvothermal route", *Thin Solid Films* **480-481**, 2005, pp. 46-49.

[13] Q. Guo, R. Agrawal, and H. Hillhouse, "Rapid Synthesis of Ternary, Binary, and Multinary Chalcogenide Nanoparticles", *PCT Int. Patent App.* WO 2008/021604 A2, 2008.

[14] C.B. Murray, C.R. Kagan, and M.G. Bawendi, "Synthesis and Characterization of Monodisperse Nanocrystals and Close-packed Nanocrystal Assemblies", *Ann. Rev. Mater. Sci.* **30**, 2000, pp. 545-610.

[15] A.L. Martinez-Skinner, M.A. Ingersoll, et. al., "Variation of indium-gallium stoichiometry in the solvothermal perparation of $CuIn_{1-x}Ga_xSe_2$ nanocrystalline materials", unpublished results -- manuscript in preparation for submission to *Chem. Mater*.

[16] E.P. Zaretskaya, V.F. Gremenok, et. al., "Raman spectroscopy of $CuInSe_2$ thin films prepared by selenization", *J. Phys. Chem. Solids* **64**, 2003, pp. 1989-1993.

[17] D. Nesheva, "Raman scattering from semiconductor nanoparticles and superlattices", *J. Optoelectronics Adv. Mater.* **7**, pp. 185-192.

[18] F. Hergert, R. Hock, et. al., "*In situ* investigation of the formation of $Cu(In,Ga)Se_2$ from selenized metallic precursors by X-ray diffraction – the impact of gallium, sodium and selenium excess", *J. Phys. Chem. Solids* **66**, 2005, pp. 1903-1907.

[19] C. Rincon and F.J. Ramirez, "Lattice vibrations of $CuInSe_2$ and $CuGaSe_2$ by Raman microspectrometry", *J. Appl. Phys.* **72**, 1992, pp. 4321-4324.

[20] T.W. Duma, F. Marsicano, and R.D. Hancock, "The affinity of gallium(III) and indium(III) for nitrogen donor ligands", *J. Coord. Chem.* **23**, 1991, pp. 221-232.

[21] F. Hergert, S. Jost, et. al., "A crystallographic description of experimentally identified formation reactions of $Cu(In,Ga)Se_2$", *J. Solid State Chem.* **179**, 2006, pp. 2394-2415.

[22]   R.N. Bhattacharya, W.K. Batchelor, et. al., "Preparation of $Cu_xIn_yGa_zSe_n$ precursor films and powders by electrodeless deposition", U.S. Patent No. 5,976,614.

[23]   T.G. Sukhova, O.N. Temkin, and R.M. Flid, "Thermodynamics of the formation of copper(I) chloride complexes", *Zhurn. Neorg. Khimii* **14**, 1969, pp. 928-931.

[24]   A.W. Atkinson, J.R. Chadwick, and E. Kinsella, "Indium-chlorine compounds", *J. Inorg. Nucl. Chem.* **30**, 1968, pp. 401-408.

[25] M.A. Carvajal, J.J. Novoa, and S. Alvarez, "Choice of coordination number in d^{10} complexes of group 11 metals", *J. Amer. Chem. Soc.* **126**, 2004, pp. 1465-1477.

[26] R.C. Weast, ed., *CRC Handbook of Chemistry and Physics, 67th ed.*, CRC Press, Inc., Boca Raton, Florida, 1986, p. D-163.

[27] M.Z. Asuncion, I. Hasegawa, et. al., "The selective dissolution of rice hull ash to form $[OSiO_{1.5}]_8[R_4N]_8$ (R = Me, CH_2CH_2OH) octasilicates. Basic nanobuilding blocks and possible models of intermediates formed during biosilification processes", *J. Mater. Chem.* **15**, 2005, pp. 2114-2121.

[28] J. Lu, Y. Xie, et. al., "Study of the dissolution behavior of selenium and tellurium in different solvents – a novel route to Se, Te tubular bulk single crystals", *J. Mater. Chem.* **12**, 2002, pp. 2755-2761.
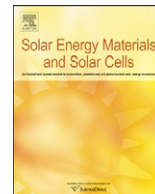
Thin films formed by selenization of CuIn$_x$B$_{1-x}$ precursors in Se vapor

C.A. Kamler [a], R.J. Soukup [a,*], N.J. Ianno [a], J.L. Huguenin-Love [a], J. Olejníček [b], S.A. Darveau [b], C.L. Exstrom [b]

[a] Department of Electrical Engineering, University of Nebraska-Lincoln, 209N WSEC Lincoln, NE 68588-0511, USA
[b] Department of Chemistry, University of Nebraska-Kearney, 905 West 25th Street Kearney, NE 68849-1150, USA

ABSTRACT

Previous attempts in producing light absorbing materials with bandgaps near the 1.37 eV efficiency optimum have included the partial substitution of gallium or aluminum for indium in the CIS system. The most efficient of these solar cells to date have had absorber layers with bandgaps < 1.2 eV. It is logical that an even smaller substitutional atom, boron, should lead to a wider bandgap with a smaller degree of atomic substitution. In this study, copper–indium–boron precursor films are sputtered onto molybdenum coated glass substrates and post-selenized. In the selenized films, although X-ray diffraction (XRD) measurements confirm that a CIS phase is present, Auger electron spectroscopy (AES) results indicate that boron is no longer homogeneously dispersed throughout the film as it was in the case of the unselenized precursor.

© 2008 Elsevier B.V. All rights reserved.

1. Introduction

A recent paper by Contreras et al. [1] has set the optimum absorber bandgap for terrestrial solar cells at 1.37 eV. In this paper they announce the highest efficiency for a chalcopyrite solar cell as 19.5%. This high efficiency is achieved with 30% Ga substitution for In within the CIGS system, yielding a bandgap of 1.14 eV. In order to attain the ideal bandgap, a substitution level of 67% Ga for In would be needed. At that level, the efficiency for CIGS solar cells is reduced to approximately 14% [1].

There are evidently several reasons for the decrease in efficiency when the Ga content becomes high enough to reach the ideal bandgap. In the above-mentioned paper the authors show that the dark current and diode ideality factor, J_0 and A, respectively, in Eq. (1) below for current density, J, as a function of developed voltage, V, both increase substantially for $E_g > 1.2$ eV:

$$J = J_0 e^{q((V-RJ)/AkT)} + GV - J_L. \qquad (1)$$

The other terms in this equation are the standard q, electron charge; k, Boltzmann's constant; R, series resistance; G, shunt conductance; and J_L, the light generated current density.

The authors explain the rise in A as a function of Ga content for all bandgaps as probably due to an increase in space charge region recombination. This increase in A is most likely due to changes in interface states between the CIGS and CdS or other window material, with more interface states for more Ga. The explanation for the increase in J_0 is probably associated with large changes in the electrical transport properties of the absorber (CIGS) layer.

This is logically due to reductions in diffusion length due to alterations in the lattice crystal structure when Ga substitution exceeds 30%. In order to achieve a 1.37 eV bandgap, a substitution of 67% Ga would be calculated from Eq. (2) below [2]:

$$E_g(x) = (1-x)E_g(A) + xE_g(B) - bx(1-x). \qquad (2)$$

In this equation A refers to In and B refers to Ga, Al, or B. (The bowing coefficient b can be shown to have little effect on the equation.) As a consequence of the high density of Ga needed to achieve the desired bandgap and the fact that the efficiency decreases when the Ga concentration exceeds 30%, attempts have been made to increase the bandgap using aluminum as a substitution for In. Using Eq. (2) above, only 25% Al would be needed to reach a bandgap of 1.37 eV.

To date, an efficiency of 16.9% has been achieved in CuIn$_{1-x}$Al$_{1-x}$Se$_2$ [3] and this is with a bandgap of about 1.15 eV with Al substituting for 13% of the In. An increase in Al content always degrades the device efficiency when compared to a CIGS cell with equal bandgap. The cause is explained to be due to significantly greater disorder in the absorber layer when the Al content is increased [4]. More recent work on this combination of materials [5] is more closely related to our efforts here. The Cu, In, and Al are deposited sequentially and selenized in an Se vapor. The resultant films do not have complete incorporation of aluminum into the CuInSe$_2$ structure, but the Al accumulates at the back of the film.

An analysis of Eq. (2) using boron and an estimate of the bandgap of CuBSe$_2$ [6] yields a substitution level for B for In of only 18.6% to yield a bandgap of 1.37 eV. Unfortunately, at this time boron has not been fully introduced into the CIS structure. An analysis of the film properties and a discussion of the methods used to produce these films are in the following section.

* Corresponding author. Tel.: +1 402 472 1980; fax: +1 402 472 4732.
E-mail address: rsoukup@unl.edu (R.J. Soukup).

2. Deposition techniques

All films fabricated in this study were deposited via magnetron sputtering of individual Cu, In, and B targets or by sputtering targets consisting of some mixture of those elements. The films were then post-selenized in a manner similar to that reported in the literature for CIGS [7,8]. Several methods were used to deposit CuInB films onto Mo coated soda-lime glass substrates:

1. Cu and $Cu_{0.45}In_{0.55}$ were DC sputtered and boron was RF sputtered. All targets were sputtered simultaneously (sample no. 070425CIB1).
2. $Cu_{0.45}In_{0.55}$ was DC sputtered and boron was RF sputtered. Both targets were sputtered simultaneously (sample no. 070718CIB1).
3. A boron layer was RF sputtered first and a $Cu_{0.45}In_{0.55}$ layer was DC sputtered onto the boron (sample no. 070427CIB1).
4. A $Cu_{0.45}In_{0.55}$ layer was DC sputtered first and boron was RF sputtered onto the $Cu_{0.45}In_{0.55}$ (sample no. 070810CIB1).
5. Cu_3B_2 and $Cu_{0.45}In_{0.55}$ targets were DC sputtered simultaneously (sample no. 070806CIB1).

Specific deposition parameters are detailed in the table. In these depositions the substrates were all at the temperature of the sputtering system with no additional heating. The layered samples are indicated by Cycles #1 and #2. The background pressure was always less than 1.3×10^{-4} Pa and all deposition took place at approximately 0.27 Pa. In each case, the substrate to target distance was 5 cm. Auger electron spectroscopy (AES) and/or XRD were used to analyze these films. The results are discussed below (Table 1).

3. Results

### 3.1. Deposition and study of precursors and selenized films

The first CIB precursor film was made by co-sputtering Cu, $Cu_{0.45}In_{0.55}$, and B. The Auger depth profile in Fig. 1 shows the atomic concentration for precursor sample 070425CIB1. The film was then subjected to an ex situ selenization procedure similar to that found in the literature for CIS [7] and CIGS [8]:

(1) The film, residing in a graphite boat with selenium reservoirs in a rough vacuum environment (~1 Pa), was heated to a temperature of 250 °C at a rate of 25 °C/min.
(2) The temperature was held at 250 °C for 20 min.
(3) The temperature was increased to 400 °C at a rate of 30 °C/min.
(4) The temperature was held at 400 °C for 30 min.

The purpose of steps 1 and 2 are to evaporate the Se to form a thin layer on the film surface. Steps 3 and 4 drive the Se into the film and allow the bonding reactions to take place. Several substrates

Table 1
Precursor deposition parameters

Sample	Sputter time (min)		Cu(0.45) In(0.55) DC current (mA)	Cu(0.4) B(0.6) DC current (mA)	Cu DC current (mA)	B RF power (W)	Cu (AES) (%)	In (AES) (%)	B (AES) (%)
	Cycle #1	Cycle #2							
070810CIB1	32 (CuIn)	225 (B)	208			150	NA	NA	NA
070806CIB1	58	NA	100	163.5			45.00	27.50	27.50
070718CIB1	98	NA	60			150	22.50	22.50	55.00
070425CIB1	186	NA	45		35	150	58.00	14.00	28.00
070228CI1	40	NA	100				45.00	55.00	0
070427CIB1	223 (B)	16 (CuIn)	100			150	NA	NA	NA
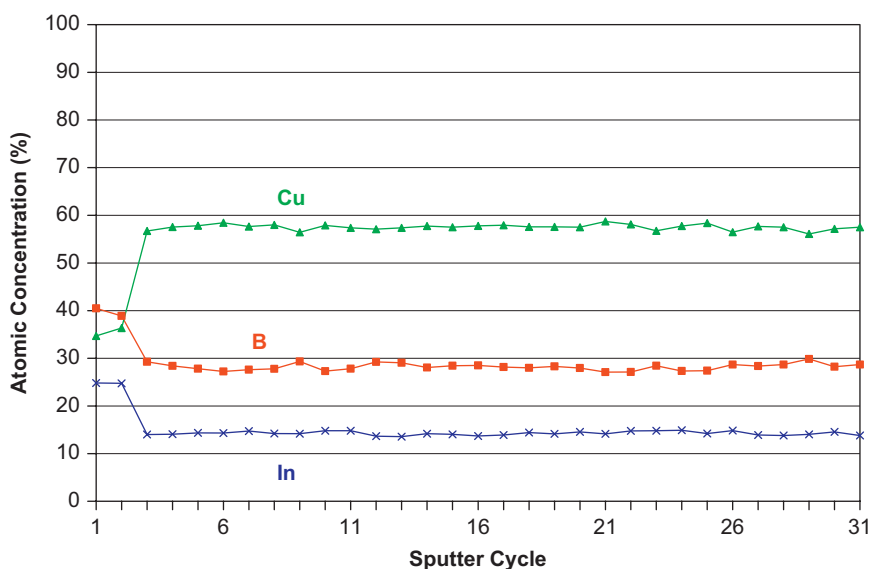
Fig. 1. Auger electron spectroscopy depth profile of a co-sputtered Cu, In, B precursor film 070425CIB1 showing uniform distribution of the atomic concentration of each element.

were deposited onto simultaneously and were subjected to different durations of the above-mentioned selenization process. XRD measurements were made on these films and the results are displayed in Fig. 2. The data depicted by the curve presented as circles is from a sample that only experienced steps 1 and 2 of the selenization process. The curve of triangles is from a sample that experienced steps 1–4 except that step 4 was shortened by 15 min. The final curve, depicted by *x*, is for a sample that fully experienced steps 1–4. Fig. 2 suggests that as the selenization procedure progresses, the film slowly changes from a Cu_2In phase, to a $Cu_{1.8}Se$ phase, to the final $CuInSe_2$ phase. Fig. 1 shows that the boron was homogenously dispersed in the precursor film.

However, Fig. 3 shows that after full selenization, boron can only be found near the back of the film. Note that in all selenized films, the AES sensitivities are uncalibrated, meaning that the depth profile measurements cannot be used to determine exact atomic percentages. AES atomic percentage analysis cannot be easily calibrated because element sensitivities change due to bonding with respect to CIXS composition. However, AES depth profile measurements taken from precursor films are calibrated; therefore these reported atomic percentages are valid.

It was thought that perhaps there was not sufficient boron sputtered into the film in order to properly synthesize CIBS, so a boron rich precursor was made (070718CIB1). The precursor film had a B concentration that was uniformly 55% throughout the film. However, as can be seen in Fig. 4 the degree of boron substitution in the precursor does not significantly affect the composition throughout most of the selenized film and the boron again is found only near the back of the selenized film.

To determine if a problem existed in the selenization process, a film of Cu and In was deposited from a $Cu_{0.45}In_{0.55}$ composite target (070228CI1). The resultant selenized film was of uniform composition throughout the film. A look at the XRD results shown in Fig. 5 shows that a selenized CuIn film does indeed form CIS.
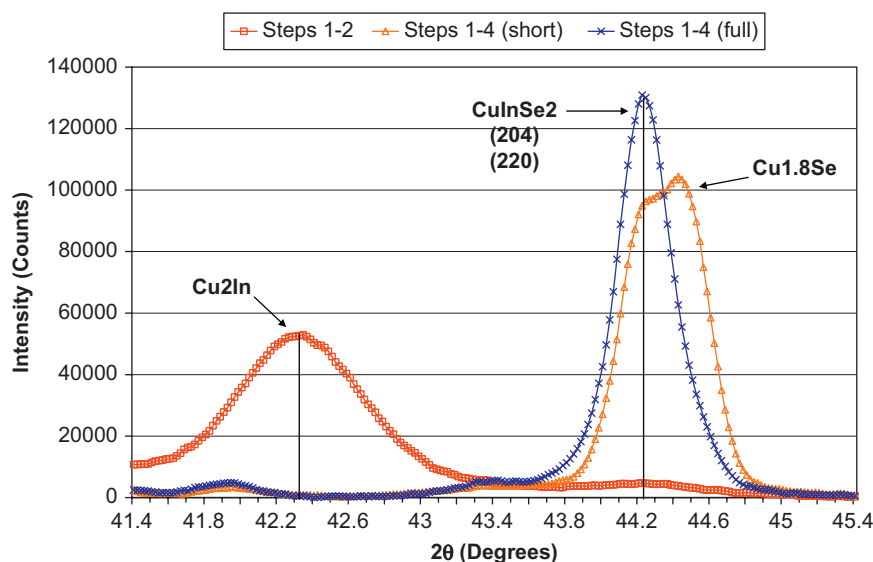

Fig. 2. X-ray diffraction of sample 070425CIB1 illustrating the shift in phase as selenization progresses.
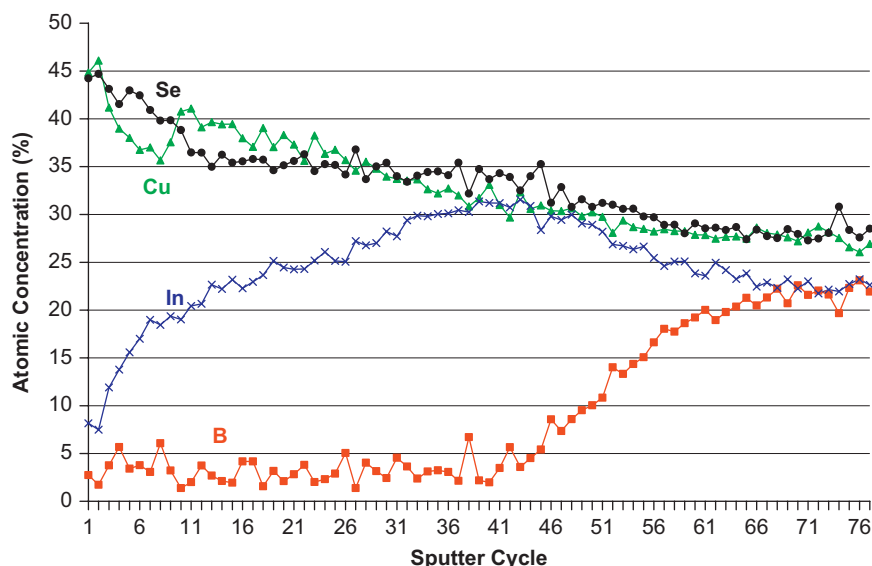

Fig. 3. Auger Electron spectroscopy depth profile of a selenized Cu, In, B precursor film 070425CIB1, illustrating the change in atomic concentration from uniformity of the as deposited film to the movement of boron to the film bottom.
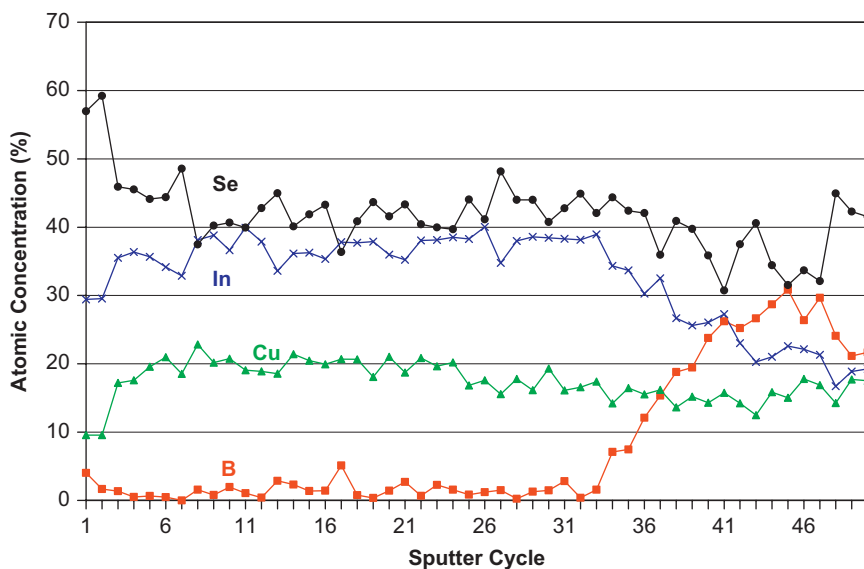
Fig. 4. Auger electron spectroscopy depth profile showing the atomic concentration of a boron rich selenized Cu, In, B precursor film 070718CIB1, with boron again accumulating at the bottom of the film.
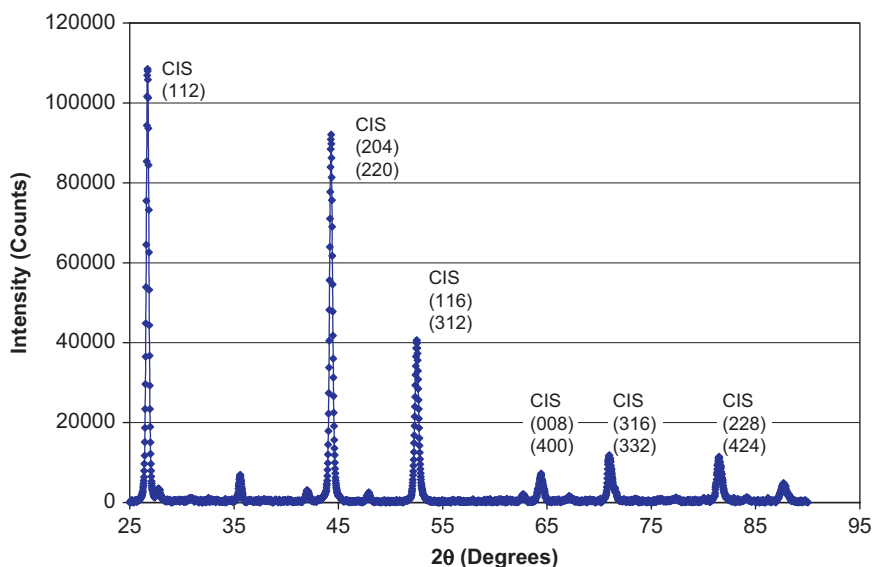

Fig. 5. X-ray diffraction results from a Cu–In film selenized using the standard procedure described in the text, the result being a CIS film, sample no. 070228CI1.

The measured 2θ are in exact agreement with the predicted values. Thus, it appears that the standard ex situ selenization procedure that is used is capable of producing quality CIS films and the problem is with the addition of boron in the precursor film.

The next precursor that was deposited consisted of a layer of CuIn sputtered on top of a layer of boron which was sputtered onto the Mo coated substrate (070427CIB1). The AES depth profile of this film was exactly as expected with a mixture of Cu and In on top of B. When this film was selenized what emerged was a layer of Cu, In, and Se on top of a layer of B. It appears that, in this case, the boron serves as a barrier to selenium penetration into the film.

In order to get a better understanding of this phenomenon the next precursor film was deposited with a layer of boron on top of a layer of CuIn on a Mo coated substrate. As expected, the AES analysis showed precursor concentrations exactly as deposited. However, AES of the selenized sample showed that a layer of Cu,

In, and Se had formed on top of a layer of B. In all probability, when this particular film was selenized, the CuIn layer diffused through the boron layer, leaving the CuInSe$_x$ layer near the surface of the film, and the boron layer at the back of the film was not selenized. This hypothesis is explained below in the description of the selenization process.

As a consequence of the unexpected nature of this result, the deposition profile was repeated. Several samples were examined after different stages in the selenization procedure in order to get a better idea of the progression of the selenization throughout the entire procedure. Fig. 6 illustrates the progression of the selenization of the films and the apparent movement of the boron through the films during selenization. Again, these samples were deposited onto simultaneously. Fig. 6a shows that after linearly elevating the temperature from room temperature to 250 °C the film is basically unchanged from the precursor, i.e. neither selenization nor atomic movement has occurred. Only a small
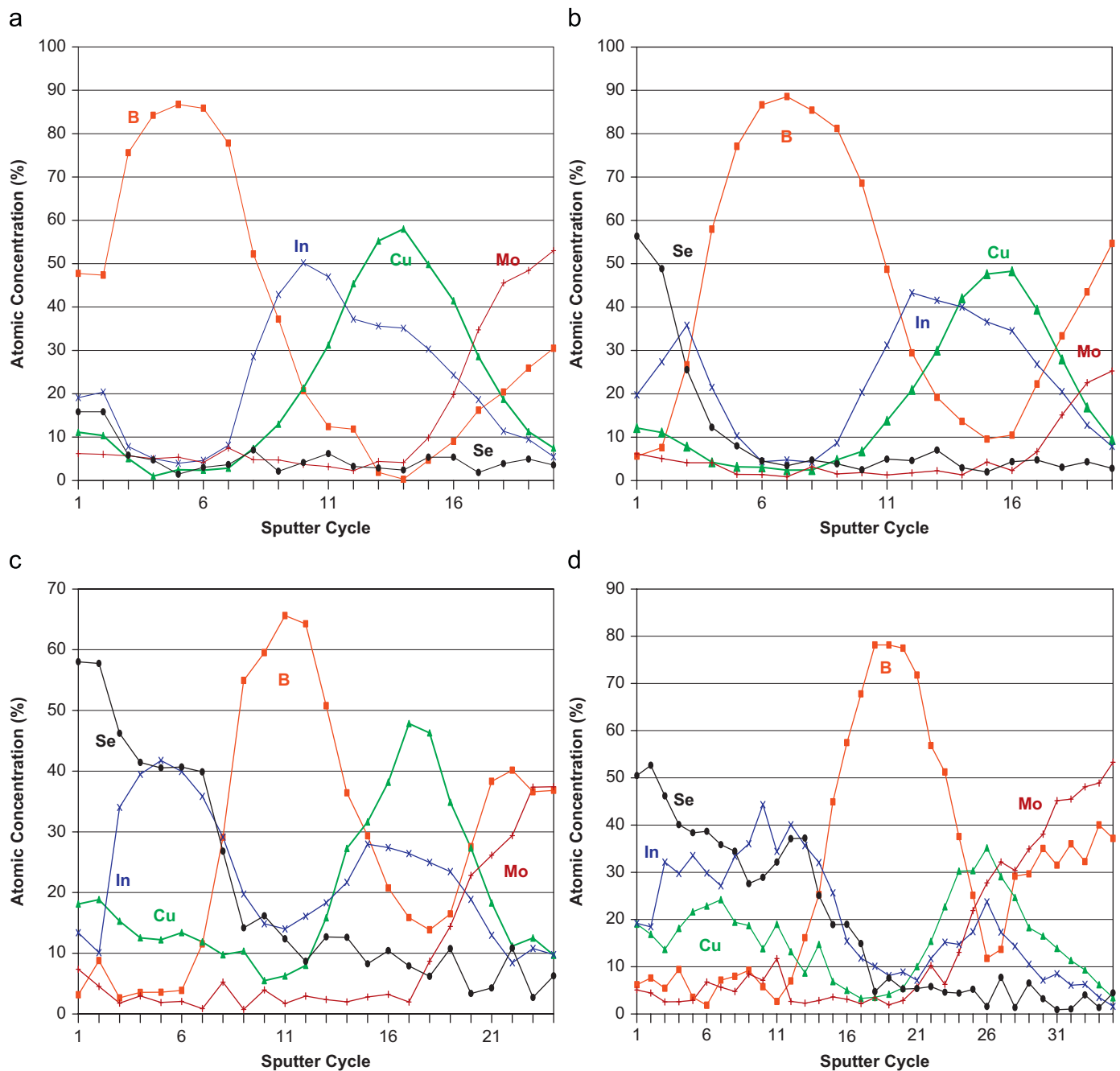
Fig. 6. (a) Auger electron spectroscopy depth profile of a selenized B on CuIn precursor. The procedure was halted immediately after the temperature was held at 250 °C for 20 min (sample 070810CIB1a). (b) AES depth profile of a selenized B on CuIn precursor. The procedure was halted immediately after a temperature ramp to 300 °C after step 2 was completed (sample 070810CIB1b). (c) AES depth profile of a selenized B on CuIn precursor. The procedure was halted immediately after a temperature ramp to 350 °C after step 2 was completed (sample 070810CIB1c). (d) AES depth profile of a selenized B on CuIn precursor. The procedure was halted immediately after a temperature ramp to 400 °C after step 2 was completed (sample 070810CIB1d).

amount of selenium can be found at the surface and none is found in the bulk of the film. However, small amounts of Cu and In have diffused to the film surface. Fig. 6b shows what the film looks like after step 2 has been completed and the process is halted after a temperature ramp to 300 °C. The only substantial difference between this stage of the process and the one preceding it is that a significant amount of Se has adhered to the film surface. The AES displayed in Fig. 6c has undergone a selenization process identical to that seen in Fig. 6b except that the temperature was ramped up to 350 °C before it was allowed to cool. This stage is almost identical to the previous one, except that the boron is now located

nearer the bottom of the film at the higher temperature. The AES displayed in Fig. 6d is for a sample which has undergone a selenization process identical to that of Fig. 6c except that the temperature was ramped up to 400 °C before it was allowed to cool.

The Auger analysis of the film represented in Fig. 6d appears to be nearly the same as one which underwent the entire standard selenization procedure. This sequence of selenization runs show that with a B on CuIn layered film, the higher the temperature and the longer the process time, the more Cu and In diffuse to the front of the film, and most of the boron appears near the back of
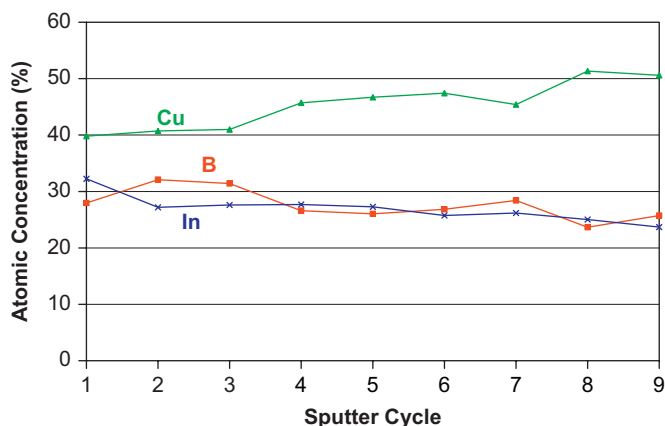
Fig. 7. The 6AES depth profile illustrating the atomic concentration of a CIB precursor made from simultaneous deposition of Cu_3B_2 and In targets (070806CIB1).

the film producing a barrier to further Se penetration. The similarity in shape of the boron for each stage of the selenization process indicates that the boron is not the diffusing element, but the Cu and In are diffusing through the boron. Once the melting point of In, $T = 156\,^{\circ}C$, has been exceeded, numerous Cu–In alloys can be in equilibrium with the molten In and substantial Cu can be dissolved in the In liquid [9] causing the molten alloy to diffuse through the boron.

In another attempt to keep the Cu and B together a CIB precursor was deposited using a Cu_3B_2 target. Although the Handbook of Chemistry and Physics [10] lists a compound Cu_3B_2, the target we purchased, expecting to receive the compound, was a mixture of Cu and B in the above ratio of 3:2. The advantage of this target is that it is able to be DC sputtered, enabling faster deposition times than with the pure B target. A precursor film made from this target along with co-sputtering of In is shown in Fig. 7. It can be seen that the ratio of Cu to B is close to the desired value initially and then the ratio of Cu to B becomes smaller. It is obvious that some experimentation with Cu_yB_z must be made before the correct film ratios can be deposited. After selenization, the film had an AES depth profile nearly identical to that of Fig. 4, again indicating that the problem is that boron is not being incorporated into the bulk of the film.

4. Conclusions

It appears that it may not be possible to form CIBS films using the precursor deposition and ex situ post-selenization method. All selenized CIBS films, whether co-sputtered from individual targets simultaneously, sputtered in layers, or sputtered from composite targets lack the presence of boron in the bulk of the film. Any boron in these films ends up in a thin region near the substrate interface. Our ability to synthesize quality CIS films using the precursor deposition/ex situ selenization suggest that the procedure is being performed as designed.

In order to more fully investigate whether CIBS films can be formed, other methods must be attempted. The next method would be to deposit the precursor films in an Se vapor as has been done successfully with aluminum [3] as the substitutional atom for indium. It may also be possible to create quality CIBS films using the hollow cathode approach [11]. Electrically excited B and Se ions that would be present in the high energy plasma may have a better chance of reacting to form B and Se bonds. The reason is that there exists a high pressure in the nozzle due to gas flow through it. Homogeneous reaction between B and Se can have high rate in comparison with cases where the pressure decreases, such as in planar magnetron sputtering. [12]

References

[1] M.A. Contreras, K. Ramanathan, J. AbuShama, F. Hasoon, D.L. Young, B. Egass, R. Noufi, Diode characteristics in state-of-the-art ZnO/CdS/Cu(In$_{1-x}$Ga$_x$)Se$_2$ solar cells, Prog. Photovolt Res. Appl. 13 (2005) 209.
[2] S.-H. Wei, A. Zunger, Band offsets and optical bowings of chalcopyrites and Zn-Based II–VI alloys, J. Appl. Phys. 78 (1995) 3846.
[3] S. Marsillac, P.D. Paulson, M.W. Haimbodi, R.W. Birkmire, W.N. Shafarman, High efficiency solar cells based on Cu(InAl)Se$_2$ thin films, Appl. Phys. Lett. 81 (2002) 1350.
[4] J.T. Heath, J.D. Cohen, W.N. Shafarman, Defects in copper indium aluminum diselenide films and their impact on photovoltaic device performance, Mat. Res. Soc. Symp. Proc. 763 (2002) B9.21.
[5] J.H. Yun, R.B.V. Chalapathy, J.C. Lee, J. Song, K.H. Yoon, Formation of CuIn$_{1-x}$Al$_x$Se$_2$ thin films by selenization of metallic precursors in se vapor, Solid State Phenom. 124–126 (2007) 975.
[6] N.J. Ianno, R.J. Soukup, T. Santero, C.A. Kamler, J.L. Huguenin-Love, S.A. Darveau, J. Olejníček, C.L. Exstrom, Copper–indium–boron–diselenide absorber materials, Mat. Res. Soc. Symp. Proc. 1012 (2007) 1012-T03-21.
[7] A.V. Mudryi, V.F. Gremenok, I.A. Victorov, V.B. Zalesski, F.V. Kurdesov, V.I. Kovalevski, M.Y. Yakushev, R.W. Martin, Optical characterization of high-quality CuInSe$_2$ thin films synthesised by two-stage selenization process, Thin Solid Films 431–432 (2003) 193.
[8] R. Caballero, C. Guillén, Optical and electrical properties of CuIn$_{1-x}$Ga$_x$Se$_2$ thin films obtained by selenization of sequentially evaporated metallic layers, Thin Solid Films 431–432 (2003) 200.
[9] N. Orbey, G.A. Jones, R.W. Birkmire, T.W.F. Russell, Copper indium alloy transformations, J. Phase Equil. 21 (2000) 509.
[10] C.D. Hodgman, R.C. Weast, S.M. Selby, Handbook of Chemistry and Physics, 39th ed, Chemical Rubber Publishing Co., 1957.
[11] R.J. Soukup, N.J. Ianno, J.L. Huguenin-Love, Analysis of semiconductor thin films deposited using a hollow cathode plasma torch, Sol. Energy Mater. Sol. Cells 91 (2007) 1383.
[12] Zdeněk Hubička, personal communication.

A non-Vacuum Process for Preparing Nanocrystalline CuIn$_{1-x}$Ga$_x$Se$_2$ Materials Involving an Open-air Solvothermal Reaction

J. Olejníček[a], C.A. Kamler[b], A. Mirasano[a], A.L. Martinez-Skinner[a], M.A. Ingersoll[a], C.L. Exstrom[a,*], S.A. Darveau[a], J.L. Huguenin-Love[b], M. Diaz[b], N. J. Ianno[b], R. J. Soukup[b]

[a] Department of Chemistry, University of Nebraska at Kearney, 905 W. 25th St. Kearney, NE 68849-1150
[b] Department of Electrical Engineering, University of Nebraska-Lincoln, 209N WSEC Lincoln, NE 68588-0511

Abstract

A non-vacuum, two-step process has been used to prepare nanocrystalline CuInSe$_2$ (CIS), CuIn$_{1-x}$Ga$_x$Se$_2$ (CIGS) and CuGaSe$_2$ (CGS) materials. An open-air solvothermal preparation in triethylenetetramine (trien) solvent was followed by annealing at 200-500 ^{o}C in a nitrogen atmosphere for 20-40 minutes. All materials have mixed clustered plate, spherical particle, and nanorod morphologies with the smallest particle diameters ranging between 20-40 nm. Raman spectroscopy, x-ray diffraction (XRD), and Auger electron spectroscopy (AES) confirm that indium/gallium ratio control is possible over a wide range. The solvothermal reaction step yields a mixture of chalcopyrite and Cu$_{2-x}$Se. This is converted to pure chalcopyrite product by annealing at 500 ^{o}C.

* Corresponding author, C. L. Exstrom, email exstromc@unk.edu, phone: 1-308-865-8565;

FAX: 1-308-865-8399

1. Introduction

For some time, the chalcopyrite semiconductors $CuInSe_2$ (CIS) and $CuIn_{1-x}Ga_xSe_2$ (CIGS) have been leading thin-film material candidates for incorporation in high-efficiency photovoltaic devices [1-4]. Interest in the development of more cost-effective, non-vacuum film production techniques has stimulated research in the solution-based preparation of nanocrystalline CIS and CIGS. Reported solvothermal preparations involve the reaction of constituent elements or their salts in heated solution for several hours or days. The solvent ethylenediamine (en) has often been employed in the preparation of binary selenides [5-7], CIS [8-11], and CIGS [10,12]. A strongly coordinating solvent, en has been proposed to solubilize reactant materials through the formation of solvent complexes such as $[Cu(en)_2]^+$ [11,12] and $[Se(en)_x]$ [13]. Reported CIS nanorod morphologies have been attributed to the square-planar geometry of $[Cu(en)_2]^+$ serving as a template for one-dimensional growth [11].

While solvothermal reactions in en may be conducted in air, required temperature conditions vary depending on the complexity of the material prepared. Binary selenides may be prepared without solvent heating [5,6], however, chalcopyrite crystalline structure formation requires elevated temperatures. CIS nanorods have been prepared from refluxing en (120 ^{o}C) [11] and several CIS and CIGS nanocrystalline samples have been prepared by superheating reaction mixtures in sealed containers at temperatures ranging from 140-280 ^{o}C [8-10,12]. Reaction temperatures in excess of 230 ^{o}C appear to be required to form CIGS nanoparticles of diameters less than 100 nm.

A two-step process consisting of a solvothermal reaction followed by heat treatment of the isolated solid product has been reported in two cases. Carmalt *et. al.* [14] solvothermally prepared CIS from CuBr, $InCl_3$, and Na_2Se in toluene, resulting in amorphous CIS that converted

to crystalline form after annealing at 500 ^{o}C for 24 hours. Li *et. al.* [5] reported unknown

"molecular precursors" following room-temperature reactions of several metals or their salts

with Se in en solvent. Heat treatments at 250 ^{o}C resulted in crystalline Ag_2Se, $CuSe$, $PbSe$,

$SnSe$, $MnSe$, Bi_2Se_3, and Sb_2Se_3, respectively.

Given that the low boiling point of en is a drawback in potential solvothermal

preparations of quaternary chalcopyrites, the use of a chemically similar solvent with a higher

boiling point may show greater promise. In this paper, we report the preparation of CIS,

$CuGaSe_2$ (CGS), and CIGS nanocrystalline materials of varying indium-gallium ratios via a two-

step process that features an open-air solvothermal reaction in refluxing triethylenetetramine

(trien) followed by annealing of the resulting solid-state product. With a molecular structure and

coordinating ability similar to en (Figure 1), trien greatly increases the utility of chelating amine

solvent use in this preparation as well as its scaleup potential. Without the need of an inert

atmosphere or necessity to exceed the normal boiling point of the solvent (267 ^{o}C), this reaction

followed by annealing in a nitrogen atmosphere at 500 ^{o}C yields CIS, CGS, and CIGS

nanocrystalline materials of varying indium-gallium ratios as characterized by scanning electron

microscopy (SEM), Raman spectroscopy, X-ray diffraction (XRD), and Auger electron

spectroscopy (AES). The reaction system shows potential for generating a variety of ternary and

quaternary chalcopyrite materials in the CIS family. To the best of our knowledge, we are the

first to report solvothermally-prepared CIGS and CGS via open-air means.

2. Experimental

Desired stoichiometric quantities of Se, $CuCl_2$, $InCl_3$, and $GaCl_3$ were refluxed in trien

for 24 (CIS) or 48 hours (CIGS, CGS). After isolation by centrifugation, rough films of the

products were cast on borosilicate glass substrates from methanol and acetone suspensions. This

was followed by annealing in a nitrogen atmosphere at 200-500 ^{o}C for 20-40 minutes. For this purpose, samples were placed in an enclosed graphite chamber that was inserted into a quartz tube surrounded by a 8000W Quad Ellipse Chamber Heater that was connected to a Model 915 power supply/temperature controller from Research, Inc. The tube was evacuated, filled with nitrogen (99.99% purity), and heated to a set-point that was varied between 200-500 °C in different experiments with a ramp rate of 8 °C/s. After annealing, the sample was cooled under flowing N_2. The product materials were characterized by micro-Raman spectroscopy (Horiba/Jon Yvon LabRAM HR800), AES (Physical Electronics 560 AES/XPS), XRD (Bruker-AXS D8 Discover), and SEM (Hitachi S4700).

3. Results and Discussion

Upon refluxing the starting materials in trien, a fine black precipitate forms within five minutes. This has been isolated and identified by micro-Raman spectroscopy and XRD as $Cu_{2-x}Se$ [15]. Over 24 (CIS) or 48 hours (CIGS, CGS) of continued refluxing, conversion to the chalcopyrite (CIS) or chalcopyrite precursors (CIGS, CGS) takes place. With added NH_4Cl in the reaction mixture, CIS reaction time is reduced to as little as 30 minutes due to competitive $[CuCl_4]^{3-}$ formation equilibria that limit $Cu_{2-x}Se$ particle growth [15]. Characterization data for all products after annealing are summarized in Table 1. CIGS product gallium content is directly proportional to the In/Ga mole ratio present in the reaction.

XRD data (Figure 2) are consistent with the tetragonal phase of the chalcopyrite crystal structure [16]. Each product shows seven orientations in expected 2θ positions for the (112), (204/220), (116/312), (400), (316/332), (442/228), and (512) crystal planes. As expected, the d(112) position shifts to higher values with increasing Ga content. The Ga/(In+Ga) ratio

estimates based on previously reported stoichiometry/lattice parameter relationships agree with the Auger analyses.

SEM images of post-annealed CIGS-1 and CGS products are shown in Figure 3. These and the other chalcopyrite materials show similar morphologies consisting of mixtures of plate-like particles or large nodules (100-400 nm in diameter), nanorods (50-100 nm diameter), and clusters of spherical nanoparticles in the diameter range of 20-40 nm each. Under the annealing conditions studied, no thin-film formation was observed.

All post-annealed products exhibit Raman spectra with single, intense scattering peaks between 172 and 185 cm^{-1} corresponding to the A_1 optical phonon mode that is characteristic of the chalcopyrite crystal structure [17]. With increasing Ga content, the peak position shifts to higher frequency and correlate to observed shifts in XRD signal positions (Figure 4). In the CIGS-3 and CGS Raman spectra, intense broad peaks are also observed in the 260-275 cm^{-1} range. Based on literature reports [18] and matching with authentic samples, this peak has been assigned to one or more $Cu_{2-x}Se$-phase impurities. Close examination of the XRD spectra of these products reveal small impurity signals at $2\theta = 44.9^o$ consistent with $Cu_{2-x}Se$ phases. Depth-profile Auger analyses indicate that the impurities reside on the particle surfaces. In the CGS sample, a separate Raman peak at 274 cm^{-1} corresponding to the chalcopyrite B_2 phonon [19] can be discerned.

Employing only the solvothermal reaction step can yield nanocrystalline CIS of reasonable quality but in CIGS and CGS preparation, there is often significant $Cu_{2-x}Se$ contamination and/or the apparent presence of metal-containing precursor solids. The latter annealing step in our two-step process serves to convert precursor solids to the chalcopyrite product and improve the crystallinity of any pre-existing chalcopyrite. To determine the effects

5

of annealing temperature on precursor conversion to chalcopyrite, the product CGS/$Cu_{2-x}Se$ mixture from a CGS solvothermal preparation reaction was isolated. Portions of this sample were annealed at 200, 300, 400, and 500 ^{o}C, respectively, for 20 minutes each. Raman spectra (Figure 5) reveal that the portion of $Cu_{2-x}Se$ converted to CGS increases with temperature, with complete conversion occurring at 500 ^{o}C or higher. Raman intensity at 185 cm^{-1} (A_1 phonon CGS) and 274 cm^{-1} (B_2 phonon of CGS) [19] slightly increases with increasing annealing temperature while the 263 cm^{-1} peak connected with several phases of $Cu_{2-x}Se$ rapidly disappears. Direct reaction of Cu_2Se and Ga_2Se_3 to form CGS is probably responsible for this behavior [20]. Similar effects were also observed for the CIGS and CIS samples.

4. Conclusion

We have developed a two-step, non-vacuum process for the preparation of CIS, CIGS, and CGS nanocrystalline materials of varying In/Ga composition ratios. An open-air solvothermal reaction of $CuCl_2$, $InCl_3$ (for CIS and CIGS only), $GaCl_3$ (for CIGS and CGS only), and Se in refluxing trien was followed by the annealing of the isolated solid product in a nitrogen atmosphere at temperatures between 200 and 500 ^{o}C. To the best of our knowledge, this is the first reported open-air solvothermal procedure employed in the preparation of CIGS and CGS materials. The high boiling point (267 ^{o}C) of trien appears to facilitate gallium incorporation into the nanocrystalline product structures. The annealing step serves to convert precursor solids to the chalcopyrite product and improve the crystallinity of any pre-existing chalcopyrite. Optimum material purity is obtained at an annealing temperature of 500 ^{o}C.

5. Acknowledgment

6. References

[1] A. Rockett, R.W. Birkmire, Copper indium selenide ($CuInSe_2$) for photovoltaic applications, J. Appl. Phys. 70 (1991), R81-R97.

[2] C. Guillen, J. Herrero, Optical properties of electrochemically deposited copper indium selenide ($CuInSe_2$) thin films, Solar Energy Mater. 23 (1991), 31-45.

[3] U. Rau, H.W. Schock, Electronic properties of $Cu(In,Ga)Se_2$ heterojunction solar cells. Recent achievements, current understanding, and future challenges Appl Phys. A: Mat. Sci. Process. 69 (1999), 131-147.

[4] A. Miguel, K. Contreras, J. Ramanathan, F. AbuShama, D.L. Hasoon, B. Young, B. Egass, R. Noufi, Diode Characteristics in State-of-the-Art $ZnO/CdS/Cu(In_{1-x}Ga_x)Se_2$ Solar Cells, Prog. Photovolt.: Res. Appl. 13 (2005), 209-216.

[5] Y. Li, Z. Wang, Y. Ding, Room temperature synthesis of metal chalcogenides in ethylenediamine, Inorg. Chem. 38 (1999), 4737-4740.

[6] W. Wang, Y. Geng, P. Yan, F. Liu, Y. Xie, Y. Qian, A novel mild route to nanocrystalline selenides at room temperature, J. Am. Chem. Soc. 121 (1999), 4062-4063.

[7] Z-H. Han, S.-H. Yu, Y.-P. Li, H.-Q. Zhao, F.-Q. Li, Y. Xie, Y.-T. Qian, Convenient solvothermal synthesis and phase control of nickel selenides with different morphologies, Chem. Mater. 11 (1999), 2302-2304.

[8] B. Li, Y. Xie, J. Huang, Y. Qian, Synthesis by a solvothermal route and characterization of $CuInSe_2$ nanowhiskers and nanoparticles, Adv. Mater. 11 (1999), 1456-1459.

[9] Y. Jiang, Y. Wu, X. Mo, W. Yu, Y. Xie, Y. Qian, Elemental solvothermal reaction to produce ternary semiconductor $CuInE_2$ (E = S, Se) nanorods, Inorg. Chem. 39 (2000), 2964-2965.

[10] K.-H. Kim, Y.-G. Chun, B.-O. Park, K.-H. Yoon, Synthesis of $CuInSe_2$ and $CuInGaSe_2$ nanoparticles by solvothermal route, Mater. Sci. Forum 449-452 (2004), 273-276.

[11] Y.-H. Yang, Y.-T. Chen, Solvothermal preparation and spectroscopic characterization of copper indium diselenide nanorods, J. Phys. Chem. B 110 (2006), 17370-17374.

[12] Y.-G. Chun, K.-H. Kim, K.-H.;Yoon, Synthesis of $CuInGaSe_2$ nanoparticles by solvothermal route, Thin Solid Films 480-481 (2005), 46-49.

[13] J. Lu, Y. Xie, F. Xu, L. Zhu, Study of the dissolution behavior of selenium and tellurium in different solvents – a novel route to Se, Te tubular bulk single crystals, J. Mater. Chem. 12 (2002), 2755-2761.

[14] C.J. Carmalt, D.E. Morrison, I.P. Parkin, Solid-state and solution phase metathetical synthesis of copper indium chalcogenides, J. Mater. Chem. 8 (1998), 2209-2211.

[15] C.L. Exstrom, S.A. Darveau, A.L. Martinez-Skinner, M.A. Ingersoll, J. Olejnicek, A. Mirasano, A.T. Haussler, J.L. Huguenin-Love, C.A. Kamler, M. Diaz, N.J. Ianno, R.J. Soukup, Reaction pathway insights into the solvothermal preparation of $CuIn_{1-x}Ga_xSe_2$ nanocrystalline materials, Proc. 33rd IEEE Photovolt. Spec. Conf., 12-16 May 2008, San Diego, CA, USA

[16] International Centre for Diffraction Data No. 40-1487.

[17] C. Rincon, F.J. Ramirez, Lattice vibrations of $CuInSe_2$ and $CuGaSe_2$ by Raman microspectrometry, J. Appl. Phys. 72 (1992), 4321-4324.

[18] V. Izquierdo-Roca, A. Perez-Rodriguez, A. Romano-Rodriguez, J.R. Morante, J. Alvarez-Garcia, L. Calvo-Barrio, Raman microprobe characterization of electrodeposited S-rich $CuIn(S,Se)_2$ for photovoltaic applications: Microstructural analysis, J. Appl. Phys. 101 (2007), 103517-1-103517-8

[19] C. Xue, D. Papadimitriou, Y.S. Raptis, Micro-Raman Study of Orientation Effect of Cu_xSe-Crystallities on Cu-rich $CuGaSe_2$ Thin Films, J. Appl. Phys. 96 (2004), 1963-1966.

[20] F. Hergert, R. Hock, A. Weber, M. Purwins, J. Palm, V. Probst, In situ investigation of the formation $Cu(In,Ga)Se_2$ from selenized metallic precursors by X-ray diffraction – The impact of Gallium, Sodium and Selenium excess, J. Phys. Chem. Solids. 66 (2005), 1903-1907.

Table 1. Characterization Data for Post-annealed $CuIn_{1-x}Ga_xSe_2$ Nanocrystalline Samples

Sample	x^a	XRD d(112), 2θ	Raman A_1 phonon, cm^{-1}
CIS	0	26.70	172
CIGS-1	0.21^b	26.74	174
CIGS-2	0.35^b	26.98	176
CIGS-3	0.79^b	27.43	179
CGS	1	27.64	185

[a] Determined by Auger spectroscopy. [b] Target x values based on starting amounts of In and Ga: 0.25 (CIGS-1), 0.50 (CIGS-2), 0.75 (CIGS-3)
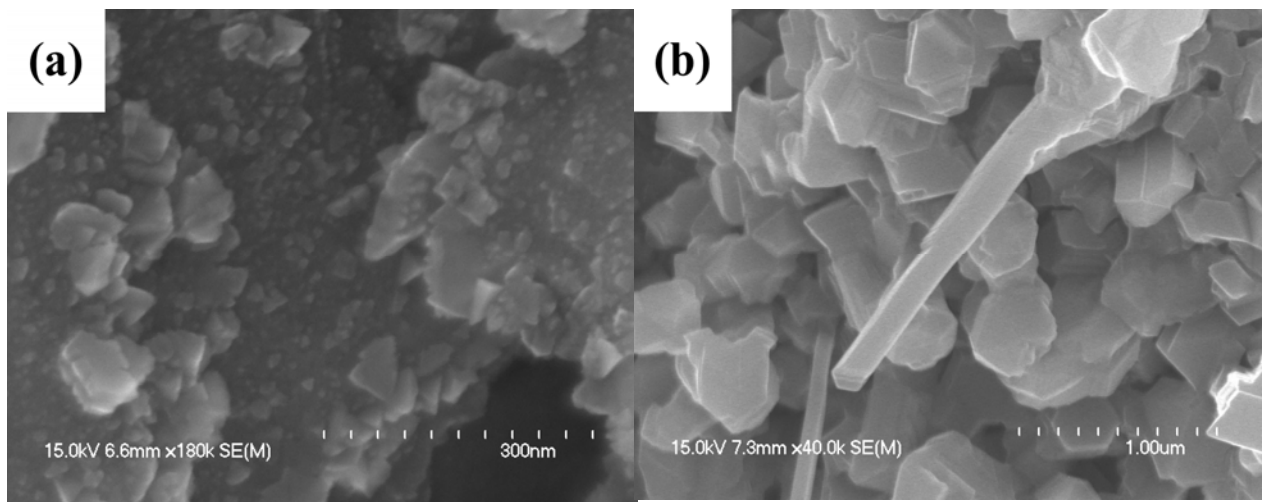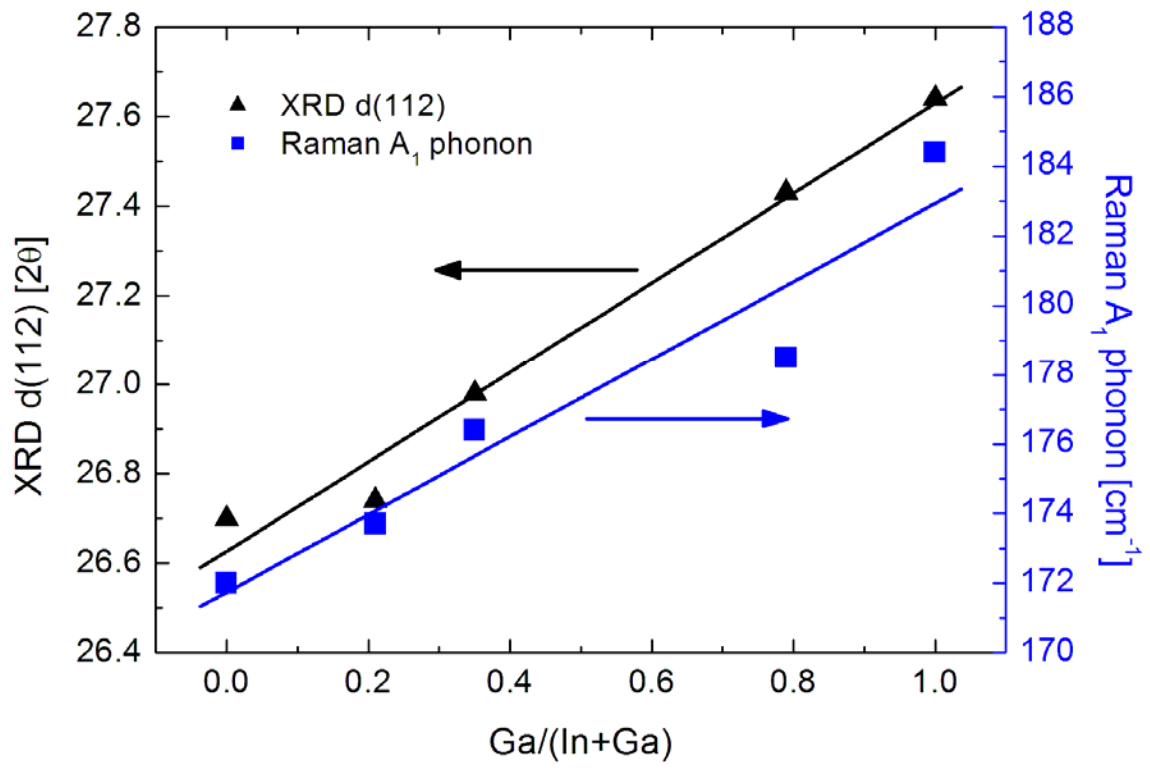
Figure 1
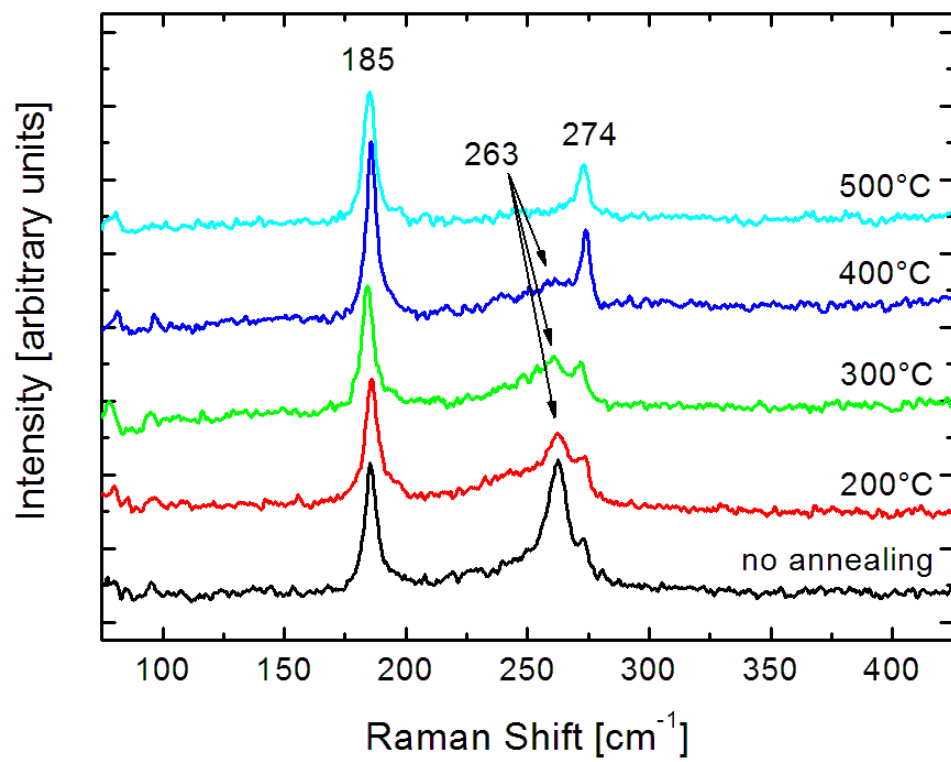
Figure 2

Figure 3

Figure 4

Figure 5

Figure Titles

1. Molecular structures of (a) ethylenediamine and (b) triethylenetetramine

2. Overlayed XRD spectra of post-annealed CIS (solid line) and CGS (dotted line) nanocrystalline samples.

3. SEM images of post-annealed (a) $CuIn_{0.79}Ga_{0.21}Se_2$ (CIGS-1 sample) and (b) $CuGaSe_2$ (CGS sample).

4. Plots of XRD d(112) angles and A_1 phonon frequencies as functions of Ga/(In+Ga) ratios in post-annealed $CuIn_{1-x}Ga_xSe_2$ materials.

5. Raman spectra of solvothermally-prepared CGS after annealing for 20 minutes at (a) 200^oC, (b) 300^oC, (c) 400^oC, and (d) 500^oC.